# RAPSYN-Mediated Neddylation of BCR-ABL Alternatively Determines the Fate of Philadelphia Chromosome-positive Leukemia

Mengya Zhao[1†], Beiying Dai[2†], Xiaodong Li[1†], Yixin Zhang[2†], Chun Qiao[2, 3], Yaru Qin[2], Zhao Li[1], Qingmei Li[1], Shuzhen Wang[1*], Yong Yang[2*], Yijun Chen[1, 2, 4*]

[1]Laboratory of Chemical Biology, School of Life Science and Technology, China Pharmaceutical University, Nanjing, 211198, China

[2]State Key Laboratory of Natural Medicines, China Pharmaceutical University, Nanjing, 211198, China

[3]Department of Hematology, The First Affiliated Hospital of Nanjing Medical University, Jiangsu Province Hospital, Nanjing, 210029, China

[4]Chongqing Innovation Institute of China Pharmaceutical University, Chongqing 401135, China

[†] These authors contributed equally

***Correspondence**: Yijun Chen (yjchen@cpu.edu.cn), Yong Yang (yy@cpu.edu.cn) and Shuzhen Wang (shuzhenwang@cpu.edu.cn)

**Abstract**

Philadelphia chromosome-positive ($Ph^+$) leukemia is a fatal hematological malignancy. Although standard treatments with tyrosine kinase inhibitors (TKI) have achieved remarkable success in prolonging patient survival, intolerance, relapse and TKI resistance remain serious issues for patients with $Ph^+$ leukemia. Here, we report a new leukemogenic process in which RAPSYN and BCR-ABL co-occur in $Ph^+$ leukemia, and RAPSYN mediates the neddylation of BCR-ABL. Consequently, neddylated BCR-ABL enhances the stability by competing its c-CBL-mediated degradation. Furthermore, SRC phosphorylates RAPSYN to activate its NEDD8 E3 ligase activity, promoting BCR-ABL stabilization and disease progression. Moreover, in contrast to *in vivo* ineffectiveness of PROTAC-based degraders, depletion of RAPSYN expression or its ligase activity decreased BCR-ABL stability and, in turn, inhibited tumor formation and growth. Collectively, these findings represent an alternative to tyrosine kinase activity for the oncoprotein and leukemogenic cells and generate a rationale of targeting RAPSYN-mediated BCR-ABL neddylation for the treatment of $Ph^+$ leukemia.

## Introduction

Philadelphia chromosome-positive ($Ph^+$) leukemia is a myeloproliferative neoplasm characterized by the reciprocal translocation between the long arms of chromosome 9 and 22, t (9;22) (q34.1; q11.2) ( de Klein et al., 1982; Deininger et al., 2000). This cytogenetic abnormality results in a *BCR-ABL* fusion gene, which encodes the chimeric protein BCR-ABL with enhanced tyrosine kinase activity (Cortes et al., 2021). Based on its oncogenic role in $Ph^+$ leukemia, BCR-ABL has been regarded as the most pivotal target for $Ph^+$ leukemia therapy, especially for chronic myeloid leukemia (CML). Tyrosine kinase inhibitors (TKI) have been the main treatment option for $Ph^+$ leukemia, remarkably prolonging the patients' life span and improving their quality of life (Hochhaus et al., 2020; Jabbour and Kantarjian, 2020). However, most patients develop TKI resistance and relapse after long-term treatment (Braun et al., 2020). It is worth noting that the increase of BCR-ABL expression can affect the sensitivity to TKIs and eventually determine the rate of TKI resistance in patients with $Ph^+$ leukemia in addition to the mutations in the kinase domain (Jabbour et al., 2007). Mutations in the kinase domain can change the conformation of BCR-ABL, thus interfering with the binding between TKIs and BCR-ABL and resulting in decreased therapeutic efficacy (Lussana et al., 2018). In parallel, the increase of BCR-ABL expression can affect the sensitivity to TKIs and eventually determine the rate of disease progression and TKI resistance in patients with $Ph^+$ leukemia (Barnes et al., 2005). Therefore, effective degradation of BCR-ABL could address the issues on TKI resistance and leukemia-initiating cells (LICs), and PROTAC-based protein degradation strategy may represent a new therapeutic approach (Bekes et al., 2022). Currently, based on different ubiquitin E3 ligases, including VHL, CRBN and IAP, PROTAC-based degraders at nM level have shown significant degradation of BCR-ABL in CML cell lines, cell lines carrying mutations in BCR-ABL as well as patient-derived primary cells containing multiple BCR-ABL mutations ( Demizu et al., 2016; Lai et al., 2016; Shimokawa et al., 2017; Zhao et al., 2019; Burslem et al., 2019; Liu et al., 2022) . Unfortunately, the excellent cellular activity by the PROTAC-based degraders

has not been able to translate to *in vivo* efficacy, even in rare examples of xenografted mouse models ( Zhao, Ren et al., 2019; Jiang et al., 2021a), resulting in uncertain usefulness of these degraders. Nonetheless, the unsatisfactory results are not really surprising because the underlying mechanism of elevated BCR-ABL expression remains largely unclear.

Receptor-associated protein of the synapse (RAPSYN) has been identified as a classic synaptic adaptor protein that binds to the acetylcholine receptor (AChR) and several cytoskeleton-associated proteins, contributing to AChR clustering and neuromuscular junction (NMJ) formation (Huh and Fuhrer, 2002; Witzemann et al., 2013). Later, RAPSYN was found to exert NEDD8 E3 ligase activity to catalyze the neddylation for AChR aggregation.(Li et al., 2016) Despite the extensive studies of RAPSYN in muscular and neuronal cells and tissues (Legay and Mei, 2017; Li et al., 2018), with regard to its involvement in leukemogenesis, there is no available information thus far except for our previous finding. Previously, RAPSYN was found to be located in the cytosol of the typical $Ph^+$ leukemia cell line K562 when a small molecule was used to probe its binding proteins using a proteomics approach (Wang et al., 2015). Because of its newly identified E3 ligase activity for neddylation and its occurrence in the $Ph^+$ leukemia cell line, we speculated that RAPSYN might contribute to $Ph^+$ leukemia development through its enzymatic activity instead of only serving as a scaffolding protein.

As a type of post-translational modification (PTM), neddylation is sequentially catalyzed by the neuronal precursor cell-expressed developmentally downregulated protein 8 (NEDD8)-activating enzyme E1 (NAE1), NEDD8-conjugating enzyme E2 (UBE2M/UBC12 or UBE2F), and a substrate-specific NEDD8 E3 ligase to complete the covalent conjugation of NEDD8 to a lysine residue of its substrates ( van der Veen and Ploegh, 2012; Enchev et al., 2015). The neddylation of proteins can be reversed by deneddylases such as NEDP1. In the last two decades, accumulating evidence indicated the strong involvement of dysregulated neddylation in tumor progression, neurodegenerative and cardiac diseases, aberrant immunoregulation and others ( Ying

111 et al., 2018; Zhou et al., 2019; Li et al., 2020; Yao et al., 2020), which rationalizes the
112 modulation of neddylation as a feasible therapeutic strategy.

113 In this study, we report that RAPSYN is highly expressed along with BCR-ABL in
114 patients with $Ph^+$ leukemia and promotes disease progression, presumably by
115 stabilizing the BCR-ABL fusion protein *via* neddylation. The neddylation of BCR-ABL
116 by RAPSYN subsequently competes its ubiquitination-dependent degradation to
117 increase the stability of BCR-ABL. Additionally, the NEDD8 E3 ligase activity of
118 RAPSYN can be substantially increased by SRC-mediated phosphorylation, leading
119 to enhanced stability and activity of RAPSYN.

120 **Results**

121 **High protein levels of RAPSYN promoted $Ph^+$ leukemia progression**

122 Prior to investigating the biological roles of RAPSYN in the pathogenesis of $Ph^+$
123 leukemia, its expression at both mRNA and protein levels was analyzed. We analyzed
124 mRNA levels of RAPSYN in RNA-seq datasets of GSE13204, GSE13159, GSE138883
125 and GSE140385, and no difference of RAPSYN mRNA levels in peripheral blood
126 mononuclear cells (PBMCs) was found between CML patients and healthy donors
127 (Figure1-figure supplement 1A). Neither a publicly available database nor our
128 collection of patient samples and cell lines showed a significant increase in mRNA
129 levels (Figure1-figure supplement 1B-C). The protein levels of RAPSYN were
130 substantially elevated in the PBMCs of $Ph^+$ CML (#8-11) and the bone marrow of ALL
131 (#7) patient samples in comparison to that of healthy donors (#1-6), which was in a
132 direct accordance with the expression of BCR-ABL (Figure 1A). This co-expression of
133 RAPSYN and BCR-ABL was also found in $Ph^+$ cell lines (Figure 1B), suggesting that
134 the function of RAPSYN in $Ph^+$ leukemia could be closely related to BCR-ABL.

135 To examine the relationship between RAPSYN and $Ph^+$ leukemia progression, we
136 first performed knockdown of its expression by using shRNAs. Whereas notable
137 cytotoxicity following marked reduction of RAPSYN was observed in all tested $Ph^+$
138 leukemia cell lines and CML patient PBMCs (Figure 1C-D, Figure1-figure supplement
139 1D-F), transduction with the shRNA for RAPSYN did not affect cell viability of

140 RAPSYN- and BCR-ABL-negative HS-5 cells, indicating the dependence on the
141 presence and expression level of BCR-ABL. Conversely, exogenous expression of
142 RAPSN rescued $Ph^+$ leukemia cells from shRNA-generated toxicity (Figure 1E).
143 Knockdown of RAPSYN also changed the phenotypes of $Ph^+$ leukemia cells, including
144 proliferation, G0/G1 cell cycle arrest and apoptosis (Figure 1-figure supplement 1G- I).
145 Next, we subcutaneously implanted sh*RAPSN* #3- or the empty vector-transduced
146 K562 cells into NCG mice to establish a cell line derived xenotransplantation mouse
147 model (Figure 1F). Tumor growth was significantly inhibited by RAPSYN silencing
148 (Figure 1G, H, Figure1-figure supplement 1J). Meanwhile, immunoblotting of tumor
149 samples showed a notable downregulation of RAPSYN expression, along with the
150 reduction of BCR-ABL levels (Figure 1I). After knockout of RAPSYN for remarkable
151 depletion of BCR-ABL expression in K562 cells (Figure 1J, Figure1-figure supplement
152 1L), these cells along with the empty vector-transduced K562 cells were intravenously
153 injected into NCG mice to establish the leukemogenic mouse model (Figure 1F).
154 Consequently, the survival of tumor-bearing mice was profoundly prolonged by the
155 knockout of RAPSYN compared to the controls (Figure 1K). Altogether, our findings
156 indicate that RAPSYN is highly expressed at protein level with the accordance to BCR-
157 ABL in $Ph^+$ leukemia and its depletion results in inhibiting the progression of $Ph^+$
158 leukemia.

159 **RAPSYN directly neddylated BCR-ABL**

160 Previous reports determined that both nicotinic AChR subunit $\alpha_7$ and muscarinic AChR
161 subtypes $M_2$, $M_3$, and $M_4$ were involved in the the cell proliferation of K562 cells
162 (Cabadak et al., 2011; Önder Narin et al., 2021). Furthermore, RAPSYN was found to
163 exert its NEDD8 E3 ligase activity toward AChR in neuronal systems (Li, Cao et al.,
164 2016). To determine whether RAPSYN functioned in a similar manner in leukemogenic
165 cells, we investigated whether RAPSYN promoted $Ph^+$ leukemia progression through
166 neddylation of AChRs. Despite the expression of AChR subunits α7, M2, M3, and M4
167 at protein level in all tested $Ph^+$ leukemia cells, no change in their neddylation was
168 observed upon RAPSYN ablation. (Figure2-figure supplement 2A, B). In addition, we

169 also examined mRNA levels of RAPSYN-related neddylation enzymes, including E1
170 (NAE1), E2 (UBE2M), NEDD8 and NEDP1, in above GSE databases, and no
171 significant differences of these neddylation-related genes were found between CML
172 patients and healthy donors as well (Figure2-figure supplement 2C). On the basis of
173 the co-expression of RAPSYN and BCR-ABL, we postulated that RAPSYN could
174 specifically mediate neddylation of BCR-ABL to promote $Ph^+$ leukemia development.

175 To test this hypothesis, reciprocal immunoprecipitation was performed to reveal a
176 strong interaction between RAPSYN and BCR-ABL in $Ph^+$ leukemia cells (Figure 2A,
177 Figure2-figure supplement 2D). Similar results were obtained with exogenous
178 expression in HEK293T cells (Figure 2B), further confirming the specific interaction of
179 RAPSYN with BCR-ABL. Furthermore, GST pull-down assay with purified proteins
180 displayed specific binding of GST-tagged RAPSYN to His-tagged BCR-ABL (Figure
181 2C), indicating that BCR-ABL is the primary target of RAPSYN-mediated neddylation.
182 Domain mapping revealed that the Δ1 domain (1-927 aa) of BCR-ABL was responsible
183 for the interaction with RAPSYN (Figure 2D).

184 Next, we studied whether RAPSYN could directly mediate BCR-ABL neddylation.
185 Strong BCR-ABL neddylation could be detected in all $Ph^+$ leukemia cell lines (Figure
186 2E, Figure2-figure supplement 2E). More importantly, the neddylation of BCR-ABL was
187 validated by immunoprecipitation using the PBMCs from two CML patients (Figure 2F).
188 Treatment with the NAE1 inhibitor, MLN4924, significantly dampened the neddylation
189 of BCR-ABL (Figure 2G, Figure2-figure supplement 2F). In addition, the mutation of
190 two glycine residues at the C-terminus of NEDD8 required for its covalent conjugating
191 ability, or the co-expression of NEDP1 (NEDD8-specific protease 1) essentially
192 diminished the neddylation of BCR-ABL (Figure 2H, I). As shown in Figure 2J, we co-
193 expressed either $RAPSYN^{WT}$ or its C366A mutant along with BCR-ABL and NEDD8,
194 revealing that mutation of Cys to Ala at the catalytic residue C366 significantly
195 decreased the neddylation level of BCR-ABL. Additionally, knockout of RAPSYN
196 abrogated BCR-ABL neddylation in the cells, and this effect was restored by
197 transduction of *RAPSN* cDNA (Figure 2K). These results were further corroborated by

198 *in vitro* experiments, which showed that BCR-ABL could hardly be neddylated in the
199 absence of RAPSYN (Figure 2L). Consistently, the amount of neddylated BCR-ABL
200 was markedly reduced in tumors generated by K562 cells transfected with
201 sh*RAPSN*#3 (Figure 2M), indicating an essential role of the ligase activity of RAPSYN
202 in BCR-ABL neddylation.

203 In addition, neither overall BCR-ABL expression nor its neddylation levels were
204 affected after the knockdown of AChRs (Figure2-figure supplement 2G). Similarly,
205 modulation of AChR activities and their downstream PKC-RAS-ERK and JAK2-AKT
206 signaling pathways ( Kawamata et al., 2011; Aydin et al., 2013) by either an agonist
207 (carbachol) (Jakubik et al., 2008) or antagonists (benzethonium and homatropine)
208 (Durieux and Nietgen, 1997) did not alter the expression or neddylation status of BCR-
209 ABL (Figure2-figure supplement 2H, I).

210 Subsequently, we tried to identified specific modification sites on BCR-ABL. The
211 purified proteins were used for *in vitro* neddylation reactions, and the target bands were
212 digested with trypsin for LC-MS/MS analyses. Eight lysine residues were found to be
213 potential NEDD8 accepting sites in BCR-ABL (Figure2-figure supplement 3). To
214 confirm these modification sites, a series of individual Lys-to-Arg mutants were
215 generated. Except for K257, neddylation levels of BCR-ABL at other candidate sites
216 were all significantly reduced, confirming the modification sites of these Lys residues
217 (Figure 2N).

218 **RAPSYN attenuated c-CBL-mediated BCR-ABL ubiquitination and degradation**

219 As decreased neddylation of BCR-ABL following either MLN4924 treatment or
220 *RAPSYN*$^{KO}$ was accompanied by a strong decline in its overall protein expression level
221 (Figure 2F, 3A-B, Figure2-figure supplement 2E, 4), we asked whether RAPSYN-
222 mediated BCR-ABL neddylation affects protein stability. Subsequently, the protein
223 synthesis inhibitor CHX was applied to K562 cells transduced with vectors encoding
224 doxycycline-inducible *RAPSN* shRNA #3. Indeed, the expression levels of BCR-ABL
225 declined much faster in cells with the induction of shRNA expression (Figure 3C).
226 Meanwhile, we found that a clear inverse correlation between the neddylation and

227 ubiquitination levels of BCR-ABL was observed (Figure 3D, E). BCR-ABL ubiquitination
228 was remarkably reduced in the cells transfected with NEDD8 (Figure 3F). Consistent
229 with these results, treatment of the cells with the proteasome inhibitor MG132
230 significantly increased the amount of ubiquitinated BCR-ABL accompanied by the
231 decrease of BCR-ABL neddylation (Figure 3G).

232 To clarify the molecular basis of the battle between BCR-ABL neddylation and its
233 ubiquitination, we detected that whether RAPSYN competes for binding to BCR-ABL
234 with c-CBL, a reported E3 ligase mediating BCR-ABL ubiquitin-proteasome
235 degradation (Mao et al., 2010). As a result, exogenous expression of RAPSYN
236 interfered with the interactions between BCR-ABL and c-CBL, whereas RAPSYN
237 ablation in K562 cells promoted c-CBL binding to BCR-ABL (Figure 3H, I). These data
238 indicated that RAPSYN competes with c-CBL for binding to BCR-ABL, leading to
239 subsequent BCR-ABL neddylation to enhance BCR-ABL stability by counteracting its
240 proteasomal degradation.

241 **SRC-mediated phosphorylation stabilized RAPSYN by repressing its**
242 **proteasomal degradation**

243 SRC-family protein tyrosine kinases are capable of phosphorylating RAPSYN in
244 neuronal system, among which SRC exerts the strongest function (Mohamed and
245 Swope, 1999). In addition, SRC has been shown to be highly expressed in primary
246 CML cells (Yang et al., 2017). We then studied whether SRC acts as an upstream
247 regulator to mediate RAPSYN. SRC inhibition with saracatinib or shRNA not only
248 significantly downregulated phosphorylated (Tyr418) SRC, but also inhibited the
249 phosphorylation of endogenous RAPSYN, resulting in a substantial decline in its
250 protein level, whereas heterologous expression of *SRC* increased RAPSYN
251 phosphorylation (Figure 4A-C, Figure4-figure supplement 5A). Furthermore, *in vitro*
252 incubation with recombinant RAPSYN, SRC, and ATP resulted in strong
253 phosphorylation of RAPSYN, which could be fully abrogated by saracatinib treatment
254 (Figure 4D). LC-MS/MS analyses indicated that Tyr residues at positions 59, 152, and
255 336 in RAPSYN are potential phosphorylation sites by SRC (Figure4-figure

256 supplement 5B). Then, after mutagenesis of these sites from Tyr to Phe, Y336, an
257 evolutionarily conserved Tyr residue, was confirmed to be the primary site of RAPSYN
258 phosphorylation (Figure 4E, Figure4-figure supplement 5C). As SRC has no effect on
259 *RAPSN* mRNA levels (Figure4-figure supplement 5D, E), implying that SRC-mediated
260 phosphorylation also affects RAPSYN stability. In fact, $Ph^+$ leukemia cells were treated
261 with saracatinib, SRC silencing or mutation of the key phosphorylation site significantly
262 accelerated the diminishment of RAPSYN expression following CHX treatment,
263 conversely, expressing exogenous SRC cDNA prolonged the half-life of RAPSYN
264 (Figure 4F-I).

265 To explore the molecular mechanisms responsible for the increased stability of
266 phosphorylated RAPSYN, $Ph^+$ leukemia cells were treated with saracatinib or
267 transduction of sh*SRC* followed by incubation with MG132. In all circumstances,
268 MG132 could rescue the decrease of RAPSYN induced by saracatinib treatment or
269 sh*SRC* knockdown (Figure 4J, K). Clearly, the specific phosphorylation of RAPSYN at
270 Y336 by SRC led to its increased stability by preventing the proteasomal degradation,
271 thereby maintaining the high levels of RAPSYN in $Ph^+$ leukemia.

272 **Phosphorylated RAPSYN potentiated its NEDD8 E3 ligase activity and promoted**
273 **BCR-ABL stabilization**

274 To dissect the role of SRC-mediated phosphorylation of RAPSYN, we tested whether
275 phosphorylation of RAPSYN at Y336 affects its ligase activity. Immunoblotting revealed
276 saracatinib treatment or SRC silencing reduced BCR-ABL neddylation and its protein
277 expression, while exogenous expression of *SRC* cDNA strongly increased it (Figure
278 5A-C). Additionally, co-expression in HEK293T cells showed that Y336F mutation had
279 no impact on BCR-ABL neddylation compared to co-transfection with SRC (Figure 5D).
280 These results were supported by stronger neddylation of endogenous BCR-ABL in
281 cells overexpressing WT RAPSYN, but not in the Y336F mutant (Figure 5E).
282 Furthermore, protein turnover rates of BCR-ABL were determined in $Ph^+$ leukemia cells
283 and the cells with exogenous $RAPSN^{Y336F}$ expression displayed larger decrease in
284 BCR-ABL level than those expressing $RAPSN^{WT}$ (Figure 5F). Therefore, RAPSYN

285 phosphorylation at Y336 by SRC was a major contributing factor to its NEDD8 E3
286 ligase activity and BCR-ABL stability in $Ph^+$ leukemia cells.

287 **Phosphorylation of RAPSYN at Y336 promoted $Ph^+$ leukemia progression**

288 To assess the extent to which SRC-mediated phosphorylation of RAPSYN at Y336
289 contributes to the enhanced viability of RAPSYN-dependent $Ph^+$ leukemia cells, we
290 first identified a specific sh*SRC* by screening five candidates using toxicity tests and
291 then performing rescue experiments with *SRC* cDNA. Toxicity tests revealed that,
292 albeit to varying degrees, sh*SRC*#2, #4, and #5 induced cytotoxicity in all $Ph^+$ leukemia
293 cell lines (Figure 6A, Figure6-figure supplement 6A). However, exogenous *SRC* cDNA
294 expression only restored the growth of $Ph^+$ leukemia cells transduced with sh*SRC*#2
295 (Figure 6B, Figure6-figure supplement 6B, C).

296 Subsequently, we performed rescue experiments by introducing $RAPSN^{WT/Y336F}$
297 cDNA or an empty vector into shSRC#2-transducted $Ph^+$ leukemia cells and found that
298 virtually complete $RAPSN^{WT}$-induced rescue was detected in both cell lines, but
299 $RAPSN^{Y336F}$ exhibited no restoring effect (Figure 6C, D). In addition, transduction of
300 $RAPSN^{WT}$ cDNA conferred an increased resistance against saracatinib treatment,
301 whereas the expression of $RAPSN^{Y336F}$ cDNA did not affect the drug sensitivity of the
302 cells (Figure 6E, F). Furthermore, knockdown of RAPSYN substantially sensitized both
303 cell lines to saracatinib (Figure 6G).

304 In animal models, while the overall survival of mice intravenously injected with
305 K562 cells expressing control empty vector was significantly improved by either
306 saracatinib administration or shRNA-mediated SRC inhibition, overexpression of WT
307 RAPSYN fully counteracted these effects and shortened the lifespan of mice to the
308 levels comparable to those of mice injected with K562 cells without SRC inhibition. In
309 contrast, expression of exogenous $RAPSN^{Y336F}$ attenuated the protective effects of
310 SRC inhibition to a much lesser extent (Figure 6H-J). Taken together, these results
311 suggest that phosphorylation at Y336 by SRC is a major event in the pro-leukemogenic
312 functions of RAPSYN in $Ph^+$ leukemia development.

313 **Discussion**

314 In this study, we identified a novel role of RAPSYN in hematology. Indeed,
315 RAPSYN inhibition significantly suppressed the survival of $Ph^+$ leukemia. This
316 phenotype was found to be linked to the NEDD8 E3 ligase activity of RAPSYN, which
317 mediated BCR-ABL neddylation to enhance its stability for promoting leukemogenesis.
318 Balanced protein synthesis and degradation are pivotal for maintaining protein
319 homeostasis and normal cellular function. Neddylation is a type of important post-
320 translational modifications (PTM) that mainly modulates protein stability. Accumulating
321 evidences have shown that targeting the neddylation process could be an appealing
322 strategy for anticancer therapy with particular efficacy in hematologic malignancies
323 (Bahjat et al., 2019; Gu et al., 2014; Guo et al., 2019; Leclerc et al., 2016; Liu et al.,
324 2018; Milhollen et al., 2010; Paiva et al., 2015; Soucy et al., 2009; Swords et al., 2018;
325 Yin et al., 2019). On the other hand, neddylation is a specific PTM that modifies multiple
326 Lys residues in BCR-ABL, shielding this oncoprotein to compete ubiquitination-
327 mediated degradation, which provides a reasonable explanation on the poor *in vivo*
328 efficacy of PROTAC-based degraders for BCR-ABL. MLN4924, a NEDD8-activating
329 E1 enzyme inhibitor, has been shown to inhibit the survival of both wild-type (WT) and
330 T315I-BCR-ABL leukemia cells as well as leukemia-initiating cells ( Liu et al., 2018;
331 Bahjat et al., 2019; Guo et al., 2019). Moreover, clinical trials of MLN4924 in
332 combination with anticancer agents in acute myeloid leukemia (AML) have progressed
333 to phase II (NCT03745352 and PEVENAZA [NCT04266795]) and III
334 (PANTHER[NCT03268954] and PEVOLAM[NCT04090736]). However, the
335 neddylation system works in a substrate- and context-dependent manner, which
336 essentially defines its role in tumorigenesis as *anti* or *pro*, particularly relying on the
337 substrate specificity of the NEDD8 E3 ligase. Neddylation can either facilitate
338 ubiquitination-dependent degradation of its substrates, such as EGFR (Oved et al.,
339 2006) and c-SRC (Lee et al., 2018), or enhance protein stability in the cases of HuR
340 (Embade et al., 2012) and TGF-β type II receptor (Zuo et al., 2013). Thus, the antitumor
341 effects of MLN4924 are the integrative outcome of inhibiting more *pro*- than *anti*-
342 tumorigenic neddylation activities in the reported tumor types. Recent studies

343 uncovered that neddylation could also inhibit tumor progression and MLN4924
344 stimulates tumor sphere formation and wound healing as well as promotes glycolysis
345 (Zhou et al., 2016; Zhou, Jiang et al., 2019; Zhou and Sun, 2019). Therefore, rather
346 than suppressing the entire neddylation system to affect a wide range of proteins,
347 targeted inhibition of substrate-specific NEDD8 E3 ligase, such as RAPSYN, might
348 offer a potential therapeutic opportunity for more elegant anticancer intervention with
349 fewer side effects.

350 Functional studies on RAPSYN have focused on its contribution to neuromuscular
351 transmission (Xing et al., 2019; Xing et al., 2020). In this study, we found that RAPSYN
352 promotes disease progression by neddylating BCR-ABL for its resistance to c-CBL-
353 mediated proteasomal degradation. Additionally, its NEDD8 E3 ligase activity was
354 incrased by SRC-mediated phosphorylation. Previously, residue of Y86 in RAPSYN
355 was identified as a phosphorylation site by muscle associated receptor tyrosine kinase
356 (MuSK) at the neuromuscular junction endplate (Xing et al., 2019), which could
357 enhance the E3 NEDD8 ligase activity of RAPSYN probably by mediating its self-
358 association (Bian et al., 2017; Koliopoulos et al., 2016; Liew et al., 2010; Metzger et
359 al., 2014; Xing et al., 2020b). Differently, we found that SRC phosphorylates RAPSYN
360 at Y336 residue located between its CC and RING domains in $Ph^+$ leukemia cells,
361 suggesting that the phosphorylation of RAPSYN might be kinase-specific or tissue-
362 specific. So far, multiple RAPSYN mutations have been reported to be causative
363 (Cossins et al., 2006; Finsterer, 2019). In particular, N88K mutation could significantly
364 reduce MuSK-mediated Y86 phosphorylation of RAPSYN to affect its E3 NEDD8
365 ligase activity (Xing et al., 2019). However, the precise process by which N88K
366 mutation is involved in modulating RAPSYN phosphorylation is unclear. On the other
367 hand, N88 was predicted to be a N-glycosylation site with the highest score among all
368 putative ones in RAPSYN (Lam et al., 2017), implicating that N-glycosylation of
369 RAPSYN could be a prerequisite for normal RAPSYN phosphorylation and activation.
370 In the present study, we unveiled that SRC-mediated RAPSYN phosphorylation could
371 substantially potentiate its NEDD8 E3 ligase activity and enhance its protein stability,

once again suggesting the hematological specificity. In addition, given the fact that neddylation and sumoylation have both shown, also in the present study, to be capable of antagonizing the ubiquitination of their substrates (Enchev et al., 2015; Yang et al., 2017b), the potential self-modification of RAPSYN is likely to promote its own stabilization. Collectively, it is of great importance to further dissect different PTMs of RAPSYN and their interactions in order to more thoroughly understand RAPSYN's biological functions.

It is well known that the generation of BCR-ABL fusion protein is a decisive characteristic of $Ph^+$ leukemia (de Klein et al., 1982). Aside from the occurrence of RAPSYN in patients with $Ph^+$ leukemia, the present study revealed a fascinating finding that BCR-ABL expression levels were correlated with those of RAPSYN, demonstrating the specificity of RAPSYN-mediated neddylation of BCR-ABL. Moreover, as a new type of PTM for BCR-ABL, RAPSYN-mediated neddylation was found to compete c-CBL-mediated ubiquitination, causing a reduction in BCR-ABL degradation. Given the fact that the increase of BCR-ABL expression can affect the sensitivity to TKIs and eventually determine the rate of TKI resistance and LIC population in patients with $Ph^+$ leukemia ( Issaad et al., 2000; Barnes, Palaiologou et al., 2005), effective degradation of BCR-ABL is an alternative opportunity for the treatment. Although recent studies have greatly advanced our understanding of the regulation of BCR-ABL degradation (Burslem, Schultz et al., 2019; Shibata et al., 2020; Jiang et al., 2021b), most reported modulatory proteins are not ideal for translation to clinical settings because of their pivotal roles in sustaining normal hematological functions. In contrast, RAPSYN was nearly unexpressed in the blood of healthy donors. Thus, it is reasonable to expect that the inhibition of RAPSYN expression could lead to cytotoxicity in $Ph^+$ leukemia with high specificity and marginal side effects. Furthermore, our present results showed that knockdown of RAPSYN significantly increased the sensitivity of leukemia cells to saracatinib, implying that a combination of RAPSYN inhibition and TKI treatment can effectively control mutations and LIC-derived TKI resistance in $Ph^+$ leukemia.

401 In summary, our work has uncovered the pivotal role that RAPSYN exerts its
402 NEDD8 E3 ligase activity in neddylating and stabilizing BCR-ABL in the pathogenesis
403 of $Ph^+$ leukemia and thus delineate it as a potential novel therapeutic target for the
404 treatment of $Ph^+$ leukemia. More importantly, our results shed a light on future
405 investigations that may help to extend to other cancer types for broadening our
406 understanding of RAPSYN's involvement in hematology and oncology.
407

408 **Materials and Methods**

409 **Human clinical samples**

410 This study was approved by the ethics committee of the First Affiliated Hospital of
411 Nanjing Medical University (2019-SR-485.A1). Human peripheral blood samples were
412 obtained from the remaining material utilized for routine laboratory tests at the First
413 Affiliated Hospital of Nanjing Medical University (Nanjing, China) and derived from 21
414 patients with $Ph^+$ chronic myeloid leukemia (CML) and six healthy volunteers. And one
415 human bone marrow sample of Ph+ acute lymphoblastic leukemia patient was
416 obtained from the remaining material utilized for routine laboratory tests at the First
417 Affiliated Hospital of Nanjing Medical University (Nanjing, China). Peripheral blood and
418 bone marrow mononuclear cells were isolated by density gradient centrifugation using
419 the Ficoll® Paque Plus solution (17-1440-02, GE Healthcare).

420 **Cell cultures**

421 K562 (female; CBP60529), MEG-01 (male; BP61104), KU812 (male; BP60732) and
422 Jurkat cells were purchased from COBIOER and cultured in Roswell Park Memorial
423 Institute 1640 medium (RPMI 1640; KGM31800, KeyGEN BioTECH) containing 10-
424 20% fetal bovine serum (FBS; FS301-02, TransGen Biotech) and 100 mg/mL
425 streptomycin/penicillin (FG101-01, TransGen Biotech). HS-5 (male; CRL11882, ATCC),
426 purchased from the American Type Culture Collection (ATCC) and HEK293T (KG405)
427 from KeyGEN BioTECH were cultured in Dulbecco's modified Eagle's medium (DMEM;
428 KGM12800, KeyGEN BioTECH) containing 10% FBS and 100 mg/mL
429 streptomycin/penicillin. All cells were cultured in a humidified incubator with 5% CO2

430 at 37°C. All the cell lines were authenticated using short tandem repeat matching
431 analysis and tested negative for mycoplasma contamination.

432 **Animal studies**

433 Female NOD/ShiLtJGpt-Prkdcem26Cd52Il2rgem26Cd22/Gpt (NCG) mice (6-8 weeks),
434 purchased from GemPharmatech Co., Ltd., were used for all in vivo studies. Mice were
435 housed under specific pathogen-free conditions at 24 ± 1°C and 55 ± 5% humidity in
436 a barrier facility with 12-h light-dark cycles. All animal experiments were performed in
437 accordance with the National Institutes of Health Guide for the Care and Use of
438 Laboratory Animals with the approval of the Center for New Drug Evaluation and
439 Research, China Pharmaceutical University (approval number: B20190925-1; Nanjing,
440 China).

441 **Apoptosis assay**

442 A total of 1-5 x $10^5$ cells were washed with phosphate-buffered saline (PBS; 02-024-
443 1ACS, Biological Industries) and resuspended in 100 μL of Annexin V binding buffer
444 (E-CK-A211, Elabscience). The cell suspension was incubated with 2.5 μL of Annexin
445 V-AF647 (E-CK-A211, Elabscience) and 2.5 μL of propidium iodide (PI; E-CK-A211,
446 Elabscience) for 20 min in the dark, followed by the addition of 400 μL of Annexin V
447 binding buffer and detection by flow cytometry (Thermo Attune NxT, MA, USA).

448 **Cell viability assay**

449 Cells were seeded at a density of 5,000 (K562) or 20,000 cells (MEG-01) per well in
450 round-bottom 96-well plates and incubated with different concentrations of saracatinib
451 (AZD0530, Selleck) or the corresponding amount of solvent for 72 h. Cells were then
452 transferred to flat-bottom 96-well plates for the determination of cell viability using the
453 CCK-8 Cell Counting Kit (A311-01, Vazyme) following the manufacturer's instructions.
454 Each experiment was performed at least three times for individual cell line.

455 **Cell proliferation assay**

456 Cells were washed twice with PBS, resuspended with a cell number of 2 x $10^6$ in 1 mL
457 PBS, and incubated with 2.5 μM carboxyfluorescein succinimidyl ester (CFSE) solution
458 (1948076, Thermo Scientific) or 5 μM carboxylic acid, acetate, and succinimidyl ester

459 (SNARF-1) solution (S-22801, Invitrogen) for 20 min at 37°C in the dark, respectively.
460 Subsequently, 1 mL of FBS was added to stop the staining, and the cells were washed
461 twice with complete media. Cell division was monitored by measuring CFSE or
462 SNARF-1 dilution using flow cytometry via channels BL1 and YL1.

463 **Cell cycle analysis**

464 A total of $1\times10^6$ cells were washed once with pre-chilled PBS, fixed in ice-cold 70%
465 ethanol, vortexing and kept for at least 20 min at -20°C. The fixed cells were washed
466 twice with PBS and stained with 20 μg/mL propidium iodide (PI) containing 100 mg/mL
467 RNAse A (740505, MACHEREY-NAGEL) for 15 min at room temperature. Stained
468 nuclei were analyzed by flow cytometry and quantified using FlowJo software (BD
469 Biosciences, NJ, USA).

470 **Cell transfection and viral transduction**

471 Transfection of the indicated DNA plasmids into HEK293T cells was performed using
472 Lipofectamine 2000 (11668500, Thermo-Fisher Scientific), according to the
473 manufacturer's instructions. Briefly, transfection of HEK293T was performed when cell
474 confluency reached 60-70%. Plasmids and Lipofectamine 2000 reagent were diluted
475 in Opti-MEM medium (31985-070, Thermo Fisher Scientific) and incubated for 5 min
476 at room temperature. They were then mixed together, incubated for another 20 min at
477 room temperature, and added to the target cells. The transfected cells were collected
478 after 48 h for further analysis.

479 **GST pull-down assay**

480 Recombinantly expressed and purified GST or GST-RAPSYN (GenBank:
481 NM_005055.5; 1236 bp ORF sequence) proteins were incubated with glutathione
482 beads 4FF (SA010010, Smart-Lifescience) overnight at 4°C in binding buffer (0.14 M
483 NaCl, 2.68 mM KCl, 2 mM $KH_2PO_4$, 0.01 M $Na_2HPO_4$, 10 mM DTT, pH 7.4), respectively,
484 and incubated with purified His-BCR-ABL (p210 BCR-ABL (b3a2); 6126 bp ORF
485 sequence) protein for another 4 h at 4°C. Beads were washed three times with washing
486 buffer (0.14 M NaCl, 2.68 mM KCl, 2 mM $KH_2PO_4$, 0.01 M $Na_2HPO_4$, 0.5 mM reduced
487 GSH, 10 mM DTT, pH 7.4), eluted with elution buffer (0.14 M NaCl, 2.68 mM KCl, 2

488 mM $KH_2PO_4$, 0.01M $Na_2HPO_4$, 10 mM reduced GSH, 10 mM DTT, pH 7.4), and
489 subjected to immunoblotting detection.

490 **Immunoblotting**

491 The cells were lysed on ice with Nonidet® P-40 (NP-40) lysis buffer (150 mM NaCl, 100
492 mM NaF, 50 mM Tris-HCl (pH 7.6), and 0.5% NP-40) supplemented with a protease
493 inhibitor cocktail (78446, Thermo Fisher Scientific). Lysates were centrifuged, quantified,
494 subjected to sodium dodecyl sulfate-polyacrylamide gel electrophoresis (SDS-PAGE), and
495 transferred to polyvinylidene difluoride (PVDF) membranes using a Bio-Rad transfer
496 apparatus. Membranes were blocked with 5% non-fat milk in Tris-buffered saline buffer
497 containing 0.1% Tween-20 (TBST) at 20-25°C for 2 h, followed by incubation with primary
498 antibody overnight at 4°C. The membranes were then washed three times in TBST buffer
499 and incubated with species-specific HRP-conjugated secondary antibodies for 2 h at room
500 temperature. Then, the membranes were washed three times in TBST buffer, developed
501 using the enhanced chemiluminescence (ECL) reagent, and exposed to the ChemiDoc
502 Imaging System (Tanon, Shanghai, China). The following antibodies were used for
503 immunoblotting or immunoprecipitation: anti-RAPSYN (ab11423, Abcam), anti-RAPSYN
504 (ab118491, Abcam), anti-6X His tag (ab18184, Abcam), anti-BCR-ABL (ab187831,
505 Abcam), anti-SRC (phosphor Y418) (ab40660, Abcam), anti-NEDD8 (#2753, Cell
506 Signaling Technology), anti-HA tag (#3724, Cell Signaling Technology), anti-GFP tag
507 (#2956, Cell Signaling Technology), anti-GST tag (#2625, Cell Signaling Technology), anti-
508 Myc tag (#2276, Cell Signaling Technology), anti-SRC (#2109, Cell Signaling Technology),
509 anti-Flag (#14793, Cell Signaling Technology), anti-GAPDH (#2118, Cell Signaling
510 Technology), anti-β-Tubulin (#2128, Cell Signaling Technology), anti-Ubiquitin (#3936, Cell
511 Signaling Technology), anti-mouse IgG, HRP-linked antibody (#7076S, Cell Signaling
512 Technology), anti-rabbit IgG, HRP-linked antibody (#7074S, Cell Signaling Technology),
513 normal mouse IgG (sc-2025, Santa Cruz Biotechnology), anti-c-CBL (sc-1651, Santa Cruz
514 Biotech), anti-AChR α7 (sc-58606, Santa Cruz Biotechnology), anti-mAChR M2 (sc-33712,
515 Santa Cruz Biotech), anti-mAChR M3 (sc-518107, Santa Cruz Biotech), anti-mAChR M4
516 (ER1906-24, HUABIO) and anti-phosphotyrosine (#05-321X, Sigma-Aldrich).

517 **Immunoprecipitation**

518 Immunoprecipitation assays were performed in accordance with the manufacturer's
519 instructions. Briefly, the cells were lysed on ice with NP-40 lysis buffer supplemented with
520 a protease inhibitor cocktail. Cell lysates were centrifuged, quantified, and incubated with
521 the appropriate primary antibody overnight at 4°C, and subsequently with protein A
522 agarose beads (16-125, Millipore) for another 4 h at 4°C. Agarose was washed three times
523 with lysis buffer and eluted with SDS-PAGE loading buffer. The eluted immunocomplexes
524 were separated by SDS-PAGE and transferred to PVDF membranes. The membranes
525 were then probed with primary and corresponding secondary antibodies, washed three
526 times in TBST buffer, developed using ECL reagent and exposed by ChemiDoc Imaging
527 System.

528 ***In vitro* neddylation assay**

529 A 30 μL reaction mixture containing 2 mM ATP-$Mg^{2+}$ (B-20, R&D), 50 ng E1
530 (APPBP1/UBA3; E-313-25, R&D), 400 ng E2 (UBE2M; E2-656-100, R&D), 0.25 μg
531 NEDD8 (UL-812-500, R&D), 0.35 μg His-BCR-ABL, with or without 4.77 μg recombinant
532 RAPSYN was incubated at 37°C for 4 h. Reaction was terminated with SDS-PAGE loading
533 buffer and assayed using immunoblotting.

534 ***In vitro* phosphorylation assay**

535 A 40 μL reaction mixture containing 2 mM ATP-$Mg^{2+}$, 3 μg recombinant RAPSYN, and
536 1 μg recombinant SRC (GenBank: NM_005417.5; 1608 bp ORF sequence) protein,
537 with or without 2 μM saracatinib (AZD0530, Selleck), was incubated at 30°C for 30 min.
538 Reaction was terminated with SDS-PAGE loading buffer and assayed by
539 immunoblotting.

540 **Animal experiments with mouse models**

541 Female NCG mice aged 6-8 weeks were used in all the animal experiments. In the
542 subcutaneous tumor experiment shown in Figure 1G, 20 mice were randomly divided
543 into two groups, followed by subcutaneous injection of $1\times10^6$ K562-shNC or K562-
544 shRAPSYN #3 cells in 60 μL Matrigel (354234, Corning) into the right foreleg. Tumor
545 size was measured every two days using a digital caliper. The tumor volume was

546 quantified using the following equation: tumor volume = 0.5 × (long diameter) × (short
547 diameter)$^2$. When the average volume of the control group exceeded 2,000 $mm^3$, the
548 mice were sacrificed. The tumors were separated, and their weights were measured.
549 As shown in the survival experiment in Figure 1J, NCG mice were inoculated with
550 K562-RAPSYN$^{WT}$ or K562-RAPSYN$^{KO}$ ($1\times10^7$ cells/mouse) via the tail vein. The
551 survival time was recorded until the mice died. As shown in the survival experiment of
552 Figure 6I, 40 mice were randomly divided into 4 groups and intravenously inoculated
553 with K562-OE-NC (20 mice), K562-OE-RAPSYN$^{WT}$ (10 mice) or K562-OE-
554 RAPSYNY$^{336F}$ (10 mice). From day 6 to 26 after tumor cell inoculation, 10 mice
555 inoculated with K562-OE-NC were treated with vehicle orally, while the other 30 mice
556 inoculated with K562-OE-NC, K562-OE-RAPSYN$^{WT}$ or K562-OE-RAPSYNY$^{336F}$, 10
557 mice in each group, were administered saracatinib orally (50 mg/kg/d). The survival
558 time was recorded until the mice died. In the survival experiment shown in Figure 6J,
559 40 mice were randomly divided into four groups and intravenously inoculated with
560 double-transfected K562 cells, as indicated. The survival time was recorded until the
561 mice died.

562 **Identification of modification sites**

563 To determine which lysine residues in BCR-ABL were neddylated by NEDD8, an *in*
564 *vitro* neddylation reaction (50 μL) was performed. After incubation at 37°C for 4 h, the
565 reaction mixture was separated by SDS-PAGE, and silver-stained bands were excised
566 and sent to BiotechPack Scientific Co., Ltd (Beijing, China) for liquid chromatography-
567 mass spectrometry (LC-MS/MS) analysis. To determine which tyrosines in RAPSYN
568 were phosphorylated by SRC, a phosphorylation reaction (50 μL) was performed. After
569 a 30 min reaction, the reaction mixture was separated by SDS-PAGE, and silver-
570 stained bands were excised and sent to Applied Protein Technology Co., Ltd.
571 (Shanghai, China) for LC-MS/MS analysis.

572 **Plasmid construction**

573 Eukaryotic expression vectors encoding His-, GST-, HA-, Myc-, or Flag-tagged
574 proteins were generated by inserting PCR-amplified fragments into the pcDNA3.1(+)

575 mammalian expression vector (V79020, Invitrogen). Eukaryotic expression vectors
576 encoding green fluorescent protein (GFP)-tagged proteins were generated by inserting
577 PCR-amplified fragments into pd1-EGFP-N1 vector (6073-1, Clontech). Prokaryotic
578 plasmids encoding GST-fusion proteins were constructed using pGEX-4T-1 bacterial
579 expression vector (27-4580-01, Addgene). Mutants of His-, HA- GST-, or GFP-tagged
580 proteins were generated using QuickMutation Site-Directed Mutagenesis Kit (D0206,
581 Beyotime) according to the manufacturer's instructions. Briefly, whole plasmid DNA
582 was amplified by PCR for 20 cycles with specific mutant primers (Supplemental Table
583 S1) using QuickMutation site-directed mutagenesis kit. Next, 1 μL DpnI was directly
584 added to the PCR reaction mixture, followed by incubation at 37°C for 30 min and
585 transformation to *E. coli* cells. To verify the mutation sites, single colonies were
586 selected for DNA sequencing and subsequent protein expression.

587 **Preparation of stable *RAPSYN*$^{KO}$ K562 cell line**

588 *RAPSYN*$^{KO}$ K562 cells were generated using CRISPR/Cas9 system (Genloci
589 Biotechnologies Inc.). Single guide RNAs for *RAPSYN* (sgRNAs) were designed using
590 online CRISPR design tool (http://crispr.mit.edu/). The sgRNA sequences were
591 ATGGGGCGCTTCCGCGTGCTGGG, GTAGCGGCCCATCTCCGAGTGGG, and
592 TCTGGTTGGACTGGTACAGCTGG, which were cloned into pGK1.1/CRISPR/Cas9
593 vector (Genloci Biotechnologies Inc.). To obtain single clones of *RAPSYN*-KO cells,
594 K562 cells were transfected with pGK1.1/CRISPR/Cas9 plasmid containing the
595 aforementioned sgRNA sequence, expanded, selected with puromycin (0120A21,
596 LEAGENE), and isolated by single-cell culturing. Single clones obtained from
597 *RAPSYN*-KO cells were validated by DNA sequencing and immunoblotting.

598 **Preparation of stable *RAPSYN*$^{KD}$ and *SRC*$^{KD}$ cell lines**

599 Lentivirus-producing shRNA targeting either human *RAPSYN* or *SRC* mRNA was used
600 to inhibit endogenous RAPSYN or SRC expression, respectively. All shRNAs
601 (Supplementary Table S1) were designed using online shRNA design tools
602 (https://rnaidesigner.thermofisher.com and https://portals.broadinstitute.org). The
603 shRNA primers were ordered from GenScript (Nanjing, China) and annealed in a

604 thermal cycler according to following procedure (95°C, 2 min; 85°C, 9 min; 75°C, 9 min;
605 65°C, 9 min; 55°C, 9 min; 45°C, 9 min; 35°C, 9 min; 25°C, 10 min; 4°C, hold) in the
606 presence of NE Buffer 2.1 (B7202S, New England BioLabs) to form a double strand
607 with EcoRI and AgeI sticky ends. Using T4 DNA ligase (M0202L, NEW ENGLAND
608 BioLabs), the double-stranded shRNAs were ligated with either lentiviral backbone
609 plasmid vector pLKO-EGFP-puro or a tet pLKO-EGFP-puro, which was digested with
610 the restriction enzymes EcoRI-HF (R3101S, NEW ENGLAND BioLabs) and AgeI-HF
611 (R3552S, NEW ENGLAND BioLabs). Plasmids containing shRNA or corresponding
612 empty vector were cotransfected with lentivirus packaging plasmids (pLP1, pLP2, and
613 pLP/VSVG) into HEK293T cells using linear polyethylenimine (23966, Polyscience)
614 transfection method. After transfection for 6–8 h, the transfection reagent was replaced
615 with a fresh medium. After incubation at 37°C, 5% $CO_2$ for 48 and 72 h, the resulting
616 lentivirus supernatant was collected respectively, and filtrated through a 0.22 μm disc
617 filter. Then, 15 mL of filtered lentivirus supernatant was concentrated through a 100
618 KDa ultrafiltration tube at 1,500 × g and 4°C for 1 h. $Ph^+$ leukemia cell lines were
619 infected with concentrated lentivirus supernatant containing 8 μg/mL polybrene (H9268,
620 Sigma). The culture plate or dish was centrifuged in a horizontal rotor centrifuge at
621 2,000 × g and 32°C for 1.5 h. After 48 h, the viral particles were replaced with fresh
622 medium, and 3 μg/mL puromycin was added for selection for another 48–72 h. Protein
623 expression levels were analyzed by immunoblotting with the antibodies of anti-
624 RAPSYN (ab118491, Abcam) or SRC (11097-1-AP, Proteintech).

625 **Preparation of stable $RAPSYN^{WT}$, $RAPSYN^{Y336F}$ or SRC expression cell lines**

626 The lentiviruses for overexpressing $RAPSYN^{WT}$, SRC (both with corresponding empty
627 vector OE-NC1) or $RAPSYN^{Y336F}$ (with corresponding empty vector OE-NC2) were
628 obtained from GenePharma Co. (Suzhou, China). The volume of virus required was
629 calculated using the following equation: $Ph^+$ leukemia cell lines were infected using the
630 spin-infection method described above. After infection for 48 h, the viral particles were
631 replaced with fresh medium. Stable $RAPSYN^{WT}$, $RAPSYN^{Y336F}$ or SRC expressing
632 cells were selected in the presence of 3 μg/mL puromycin for 48-72 h. Protein

633 expression levels were analyzed by immunoblotting with anti-RAPSYN or anti-SRC
634 antibodies.

635 $$\text{virus volume} = \frac{\text{MOI} \times \text{cell number}}{\text{virus titer}}$$

636 **Protein expression and purification**

637 Recombinant pGEX-4T-1-GST-RAPSYN plasmid were transformed into the
638 ArcticExpress (DE3) pRARE2 competent *E. coli* cells (AYBIO-G6023, ANGYUBIO)
639 and treated with 0.4 mM isopropyl-β-D-thiogalactoside (367-93-1, Sangon Biotech) to
640 induce fusion protein expression at 18°C. After the induction for 50 h, bacterial cells
641 were harvested, resuspended in PBS (0.14 M NaCl, 2.68 mM KCl, 2mM $KH_2PO4$,
642 0.01M $Na_2HPO_4$, 10 mM DTT, pH 7.4), and sonicated on ice. Precipitates were
643 removed from cell lysates by centrifugation. Recombinant GST-RAPSYN was purified
644 from the supernatant by GST-affinity chromatography (SA010010, Smart-Lifescience)
645 and size-exclusion chromatography (17-0060-01, GE Healthcare). Purified GST-
646 RAPSYN protein was digested with thrombin (T8021, Solarbio) for 6 h at 4°C to remove
647 GST tag. Recombinant pcDNA3.1-His-BCR-ABL plasmids were transfected into
648 HEK293T cells and were collected after 48 h culturing. The cells were then lysed on
649 ice using Nonidet P-40 (NP-40) lysis buffer with a protease inhibitor cocktail. Cell
650 lysates were centrifuged, and then the supernatant fraction was incubated with anti-
651 BCR-ABL antibody overnight at 4°C and subsequently with protein A magnetic beads
652 (73778, Cell Signaling Technology) for another 4 h at 4°C. The bead complexes were
653 washed three times with washing buffer (25 mM Tris-HCl, 0.15 M NaCl, 0.005%
654 Tween-20, pH 7.5), eluted with elution buffer (0.1 M glycine, pH 2.0), and mixed with
655 neutralization buffer (1 M Tris-HCl, pH 9.0) for neutralization of purified protein.

656 **Protein stability assay**

657 $RAPSYN^{WT}$, $RAPSYN^{Y336F}$, or BCR-ABL-transfected $Ph^+$ leukemia cells were
658 incubated with 100 mg/mL cycloheximide (CHX, A8244; Cell Signaling Technology)
659 for indicated time points. Cells were harvested and lysed on ice using NP-40 lysis
660 buffer supplemented with a protease inhibitor cocktail. The supernatant was collected
661 and subjected to immunoblotting using anti-RAPSYN or anti-SRC antibodies.

662 **Quantitative reverse transcription-PCR (RT-PCR)**

663 High-quality RNA was isolated from cells or tissues using Trizol reagent (AJF1807A,
664 Takara) according to the manufacturer's instructions. cDNA was synthesized from 1
665 μg of total RNA using HiScriptIIRT SuperMix for qPCR (R233-01, Vazyme). The
666 ChamQ SYBR qPCR Master Mix (Q331-02, Vazyme) was used for two-step RT-PCR
667 analysis on an Applied Biosystems StepOnePlus Real-Time PCR instrument. The
668 samples were analyzed in triplicate. The expression value of target gene in a given
669 sample was normalized to the corresponding expression of ACTB or GAPDH. The $2^{-\Delta\Delta Ct}$
670 method was used to calculate relative expression of target genes. The primers
671 used are listed in Supplementary Table S1.

672 **Cytotoxicity assay**

673 Lentiviruses co-expressing GFP were used to assess the toxicity of shRNAs. Flow
674 cytometry was performed two days after shRNA transduction to determine initial GFP-
675 positive proportion of live cells for each shRNA. Subsequently, the cells were sampled
676 every two days over the time. The GFP-positive proportion at each time point was
677 normalized to that of day two. Each shRNA experiment was performed at least three
678 times for individual cell line.

679 **Statistical analysis**

680 All *in vitro* experiments were repeated at least three times. Animals were randomly
681 assigned to different groups for each *in vivo* study. Kaplan-Meier survival analysis was
682 used for all survival studies, and the log-rank test was used to determine significant
683 differences between groups. Differences with * $p < 0.05$, ** $p < 0.01$, *** $p < 0.001$, and
684 **** $p < 0.0001$ were considered significant. Prism 8 (GraphPad Software, CA, USA)
685 was used for statistical analysis. Representative results from at least three
686 independent replicates are shown. Data are presented as mean ± SD, and significant
687 differences were determined using Student's t test, unpaired Student's t test, or one-
688 way analysis of variance test.

689

690 **Acknowledgements**

This work was supported by the grants of National Key R&D Program of China (2018YFA0902000), National Science Foundation of China (No. 81872924, 81973386 and 82002971), “Double First-Class” University Project (CPU2022QZ014), Project Program of the State Key Laboratory of Natural Medicines, China Pharmaceutical University (SKLNMZZ202201) and PAPD of Jiangsu Province.

## Additional information

### Funding


| Funder | Grant reference number | Author |
|---|---|---|
| National Natural Science Foundation of China | 81973386 | Yijun Chen |
| National Natural Science Foundation of China | 81872924 | Shuzhen Wang |
| National Natural Science Foundation of China | 82002971 | Beiying Dai |
| National Key R&D Program of China | 2018YFA0902000 | Yijun Chen |
| “Double First-Class” University Project | CPU2022QZ014 | Yijun Chen |
| Project Program of the State Key Laboratory of Natural Medicines | SKLNMZZ202201 | Yijun Chen |
| Key Research and Development Project of Guangdong Province | 2022B1111070004 | Yijun Chen |

The funders had no role in the study design, data collection and interpretation, or the decision to submit the work for publication.


### Author contributions

Mengya Zhao, Formal analysis, Investigation, Data curation, Methodology, Writing - original draft; Beiying Dai, Formal analysis, Investigation, Data curation, Methodology,

Writing - original draft, Project administration, Funding acquisition; Xiaodong Li, Formal analysis, Investigation, Data curation, Methodology; Yixin Zhang, Formal analysis, Investigation, Data curation, Methodology; Chun Qiao, Data curation; Yaru Qin, Data curation; Qingmei Li, Data curation; Zhao Li, Data curation; Shuzhen Wang, Supervision, Project administration, Funding acquisition, Writing - review & editing; Yong Yang, Supervision, Resources; Yijun Chen, Conceptualization, Supervision, Resources, Writing - review & editing, Funding acquisition.

**Competing interests**

A Chinese patent application was filed with the number of 202210107464.7. China Pharmaceutical University owns the patent rights, and Y. C., Y. Y., M. Z., B. D., X. L., S. W. and X. Z. are the inventors of the patent.

**Data availability**

The data generated in this study are available upon request from the corresponding authors.

**Ethics**

This study was approved by the ethics committee of the First Affiliated Hospital of Nanjing Medical University (2019-SR-485.A1). All animal experiments were performed in accordance with the National Institutes of Health Guide for the Care and Use of Laboratory Animals with the approval of the Center for New Drug Evaluation and Research, China Pharmaceutical University (approval number: B20190925-1; Nanjing, China).

## Figures and figure legends

Figure 1

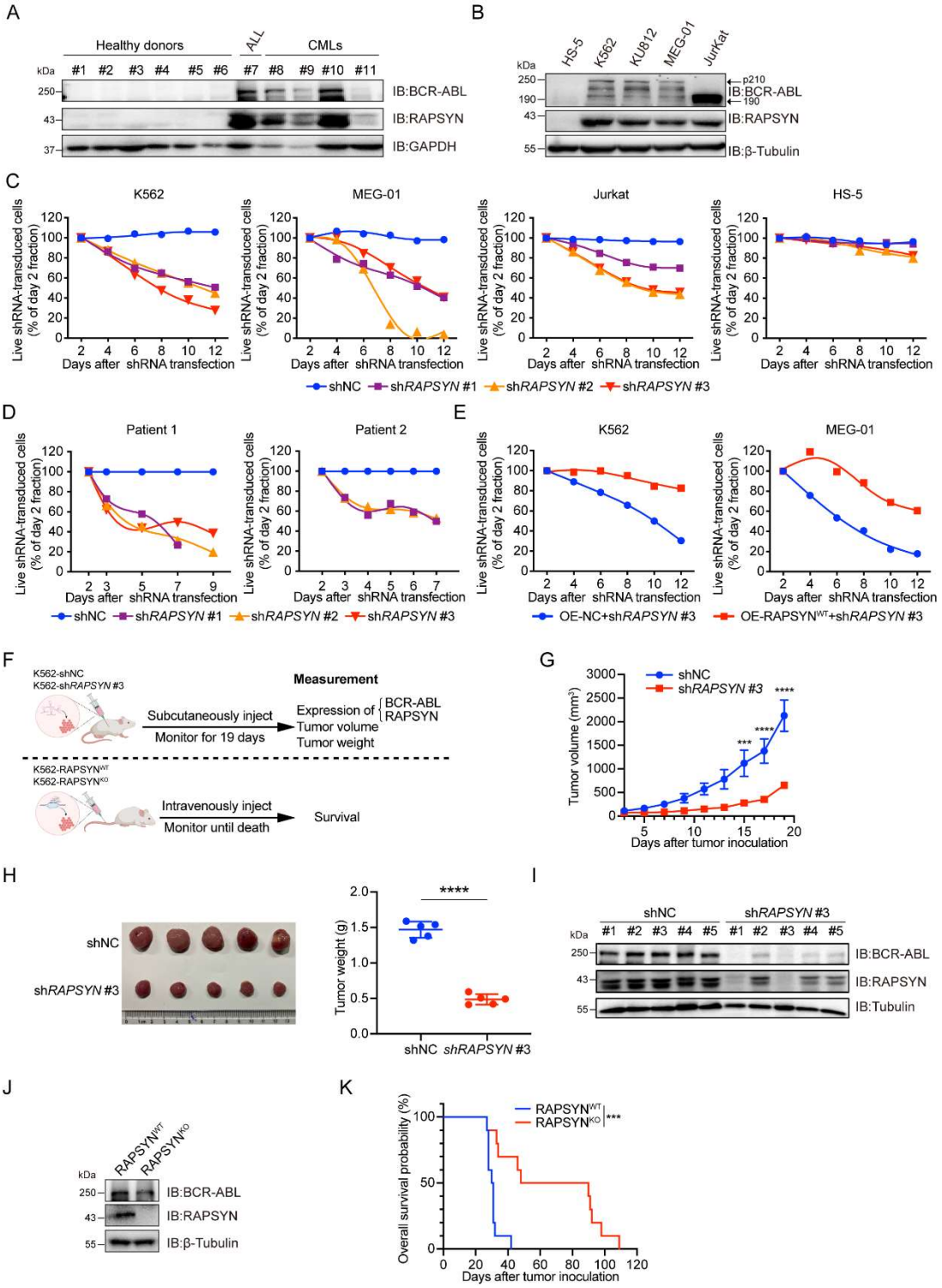


**Figure 1. High protein levels of RAPSYN promotes Ph⁺ leukemia progression.**

(A) Immunoblots of RAPSYN and BCR-ABL in the peripheral blood mononuclear cells

731 (PBMCs) of clinical samples.

732 (B) Immunoblots of RAPSYN and BCR-ABL in $Ph^+$ leukemic cells and normal bone
733 marrow stromal cells (HS-5).

734 (C) Cytotoxicity induced by shRNA-mediated RAPSYN knockdown in leukemic and
735 HS-5 cells.

736 (D) Cytotoxicity induced by shRNA-mediated RAPSYN knockdown in the PBMCs of
737 CML patients.

738 (E) Rescue of leukemic cells from sh*RAPSN* #3-induced toxicity by exogenous
739 expression of RAPSN cDNA.

740 (F) An *in vivo* experimental design for testing the effects of RAPSYN on tumor growth
741 and survival.

742 (G) The growth curve of subcutaneous xenograft tumors was measured every two days
743 from the third day after tumor inoculation for 19 days (five mice in each group).

744 (H) Photograph and weight quantification of excised tumor xenografts from (I).

745 (I) Immunoblots of RAPSYN and BCR-ABL in mouse xenograft tumor biopsies from
746 K562 cells transduced with sh*RAPSN* #3 or shNC.

747 (J) Immunoblots of RAPSYN and BCR-ABL in K562-$RAPSYN^{WT}$ and K562-$RAPSYN^{KO}$
748 cells.

749 (K) Kaplan-Meier survival curve of NCG mice following intravenous injection of K562-
750 $RAPSYN^{WT}$ or K562-$RAPSYN^{KO}$ cells, as shown in (H) (ten mice in each group).

751 All data represent mean ± SD of at least three independent experiments. *P* values
752 were calculated using unpaired Student's t-test or log-rank test. * $p < 0.05$, ** $p <$
753 $0.01$, *** $p < 0.001$, **** $p < 0.0001$.

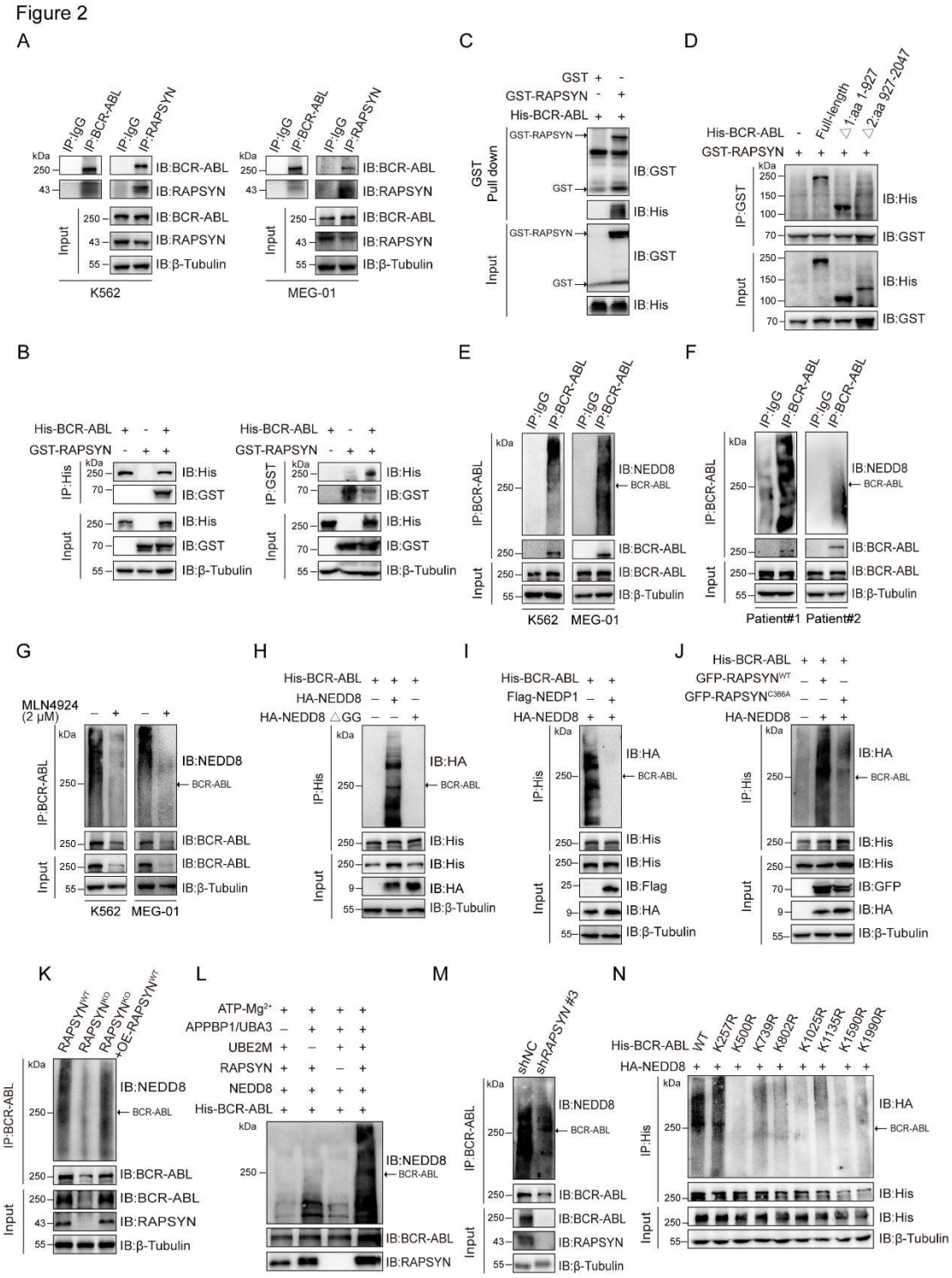


754

755 **Figure 2. RAPSYN neddylates BCR-ABL.**

756 (A) Co-immunoprecipitation of BCR-ABL and RAPSYN in leukemic cells.

757 (B) Immunoblots of GST and His after immunoprecipitation of His or GST in HEK293T

758 cells transfected with His-tagged BCR-ABL and GST-tagged RAPSYN.

759 (C) Immunoblots of GST and His following GST pull-down after *in vitro* incubation of

760 purified His-tagged BCR-ABL and GST or GST-tagged RAPSYN.

761 (D) His-immunoblots of GST immunoprecipitates from HEK293T cells transfected with
762 GST-tagged RAPSYN alone or in combination with His-tagged full-length or truncated
763 BCR-ABL (Δ1: aa 1-927, Δ2: aa 928-2047).

764 (E) Analysis of BCR-ABL neddylation levels in leukemic cells.

765 (F) Analysis of BCR-ABL neddylation levels in the PBMCs of CML patients.

766 (G) Analysis of BCR-ABL neddylation levels in leukemic cells treated with MLN4924 or
767 DMSO for 24 h.

768 (H) HA-immunoblots of His-immunoprecipitate from HEK293T cells transfected with
769 His-tagged BCR-ABL and HA-tagged NEDD8 or NEDD8 ΔGG.

770 (I) HA-immunoblots of His-immunoprecipitate from HEK293T cells transfected with
771 indicated constructs.

772 (J) Analysis of BCR-ABL neddylation levels in K562 WT, RAPSYN-KO and RAPSYN-
773 KO with exogenous expression of a RAPSN cDNA cells.

774 (K) HA-immunoblots after immunoprecipitation of His-antibody in HEK293T cells
775 transfected with His-tagged BCR-ABL, HA-tagged NEDD8, GFP-tagged WT RAPSYN
776 or RAPSYN-C366A.

777 (L) Assessment of BCR-ABL neddylation by RAPSYN *in vitro* enzymatic reactions.
778 Recombinantly expressed and purified RAPSYN and BCR-ABL were incubated with
779 APPBP1/UBA3, UBE2M or NEDD8 for *in vitro* neddylation assay.

780 (M) Analysis of BCR-ABL neddylation levels in excised tumor xenografts from Fig. 1H.

781 (N) Verification of BCR-ABL neddylation sites in HEK293T cells transfected with
782 indicated constructs.

783

Figure 3

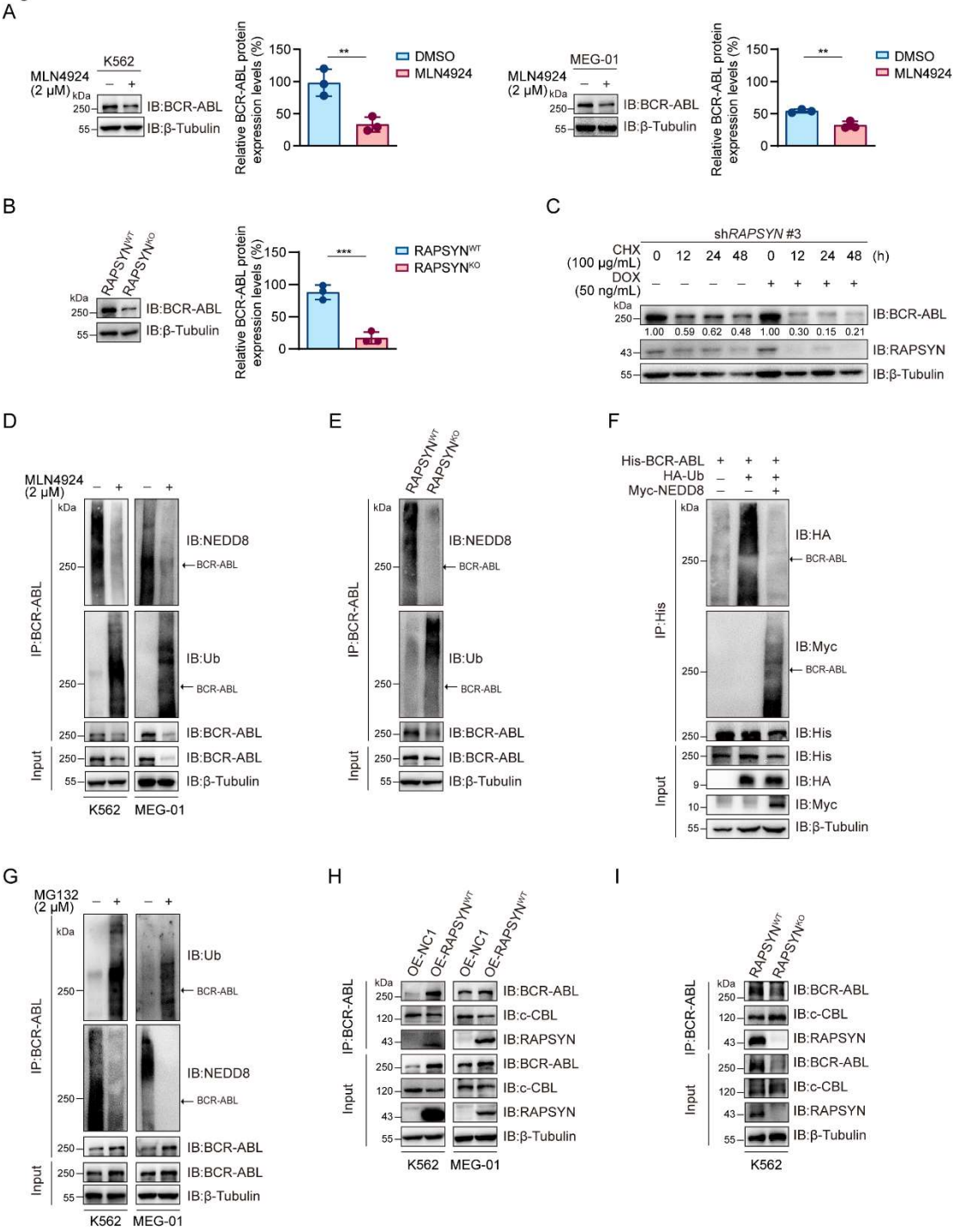


**Figure 3. RAPSYN attenuates BCR-ABL ubiquitination and degradation.**

(A) Immunoblots of BCR-ABL in leukemic cells treated with MLN4924 or DMSO for 24 h and corresponding quantification of three independent replicates.

(B) Immunoblots of BCR-ABL in K562 WT and RAPSYN-KO cells and corresponding quantification of three independent replicates.

790 (C) Assessment of BCR-ABL protein stability in K562 cells expressing DOX-inducible
791 sh*RAPSN* #3 treated with CHX alone or in combination with DOX at indicated time
792 points by immunoblotting.
793 (D) Analysis of BCR-ABL neddylation and ubiquitination levels in leukemic cells treated
794 with MLN4924 or DMSO for 24 h.
795 (E) Analysis of BCR-ABL neddylation and ubiquitination levels in K562 WT and
796 RAPSYN KO cells.
797 (F) Immunoblots of HA and Myc after His-immunoprecipitation in HEK293T cells
798 transfected with His-tagged BCR-ABL, HA-tagged Ub or without Myc-tagged NEDD8.
799 (G) Analysis of BCR-ABL ubiquitination and neddylation in leukemic cells treated with
800 MG132 or DMSO for 12 h.
801 (H) Co-immunoprecipitation of BCR-ABL, c-CBL and RAPSYN in leukemic cells
802 expressing exogenous RAPSN cDNA or empty vector.
803 (I) Co-immunoprecipitation of BCR-ABL, c-CBL and RAPSYN in K562 WT and
804 RAPSYN KO cells.
805 All data represent mean ± SD of at least three independent experiments. P values were
806 calculated using unpaired Student's t-test. ** $p < 0.01$, *** $p < 0.001$.

Figure 4

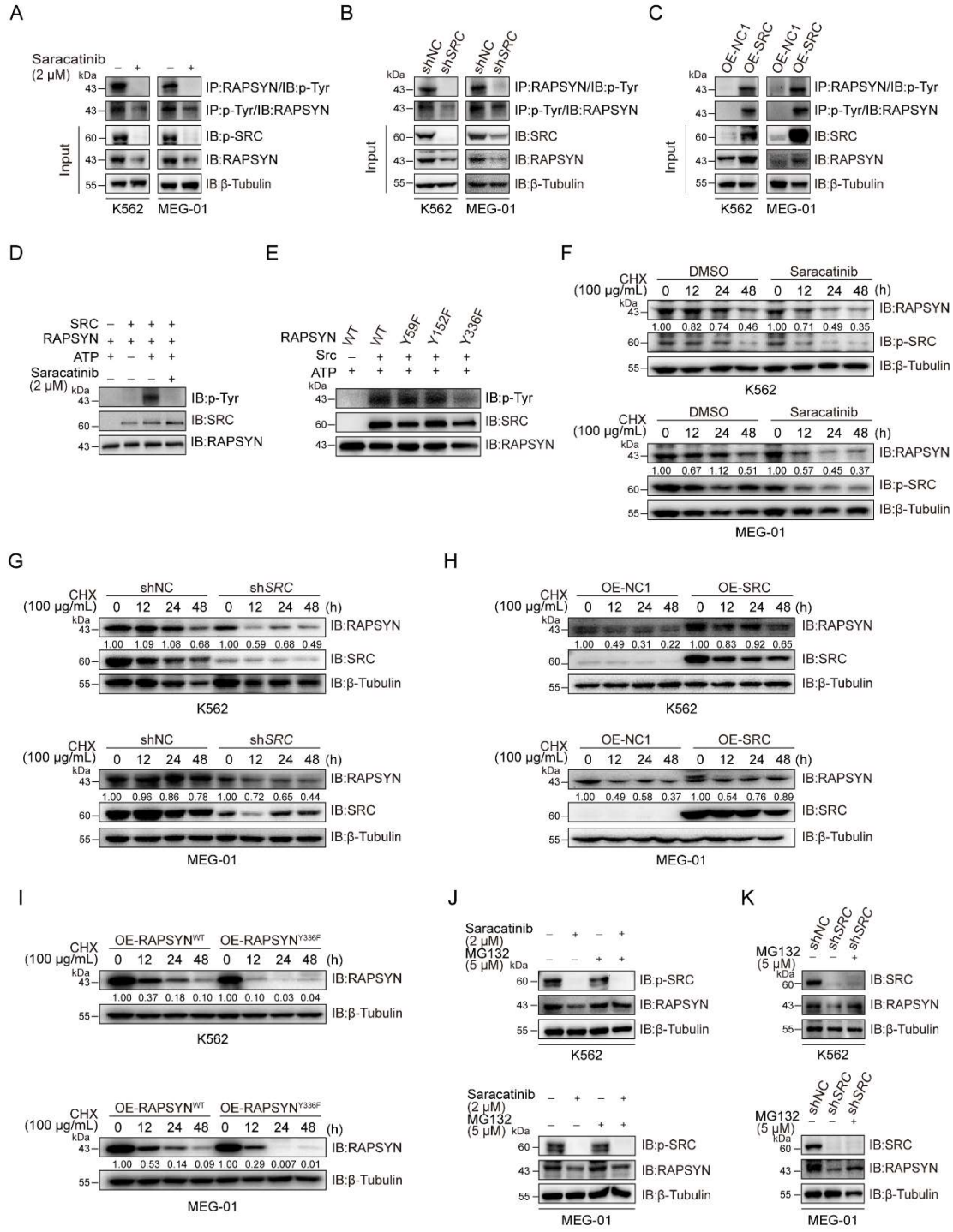


**Figure 4. SRC-mediated phosphorylation at Y336 promotes RAPSYN stability by repressing its proteasomal degradation.**

(A) Assessment of RAPSYN phosphorylation levels in leukemic cells treated with saracatinib or DMSO for 24 h.

(B) Assessment of RAPSYN phosphorylation levels in leukemic cells transduced with

813 shSRC or shNC.

814 (C) Assessment of RAPSYN phosphorylation levels in leukemic cells expressing
815 exogenous SRC cDNA or empty vector.

816 (D) Assessment of RAPSYN phosphorylation by SRC in vitro. Purified RAPSYN and
817 SRC were incubated with ATP in the presence or absence of saracatinib for
818 phosphorylation assay.

819 (E) Verification of RAPSYN phosphorylation sites. Purified SRC and RAPSYN WT or
820 indicated mutants were incubated with ATP for phosphorylation assay.

821 (F) Assessment of RAPSYN protein stability in leukemic cells treated with CHX in
822 combination with saracatinib or DMSO at indicated time points by immunoblotting.

823 (G) Assessment of RAPSYN protein stability in leukemic cells transduced with shSRC
824 or shNC by immunoblotting.

825 (H) Assessment of RAPSYN protein stability in leukemic cells transduced with
826 exogenous SRC cDNA or empty vector by immunoblotting.

827 (I) Assessment of RAPSYN protein stability in leukemic cells transduced with
828 exogenous RAPSYN WT or Y336F cDNA by immunoblotting.

829 (J) Immunoblots of RAPSYN in leukemic cells treated with saracatinib or DMSO for 12
830 h, and subsequently with MG132 or DMSO for another 12 h.

831 (K) Immunoblots of RAPSYN in leukemic cells transduced with shNC or shSRC and
832 treated with MG132 or DMSO for 12 h.

Figure 5

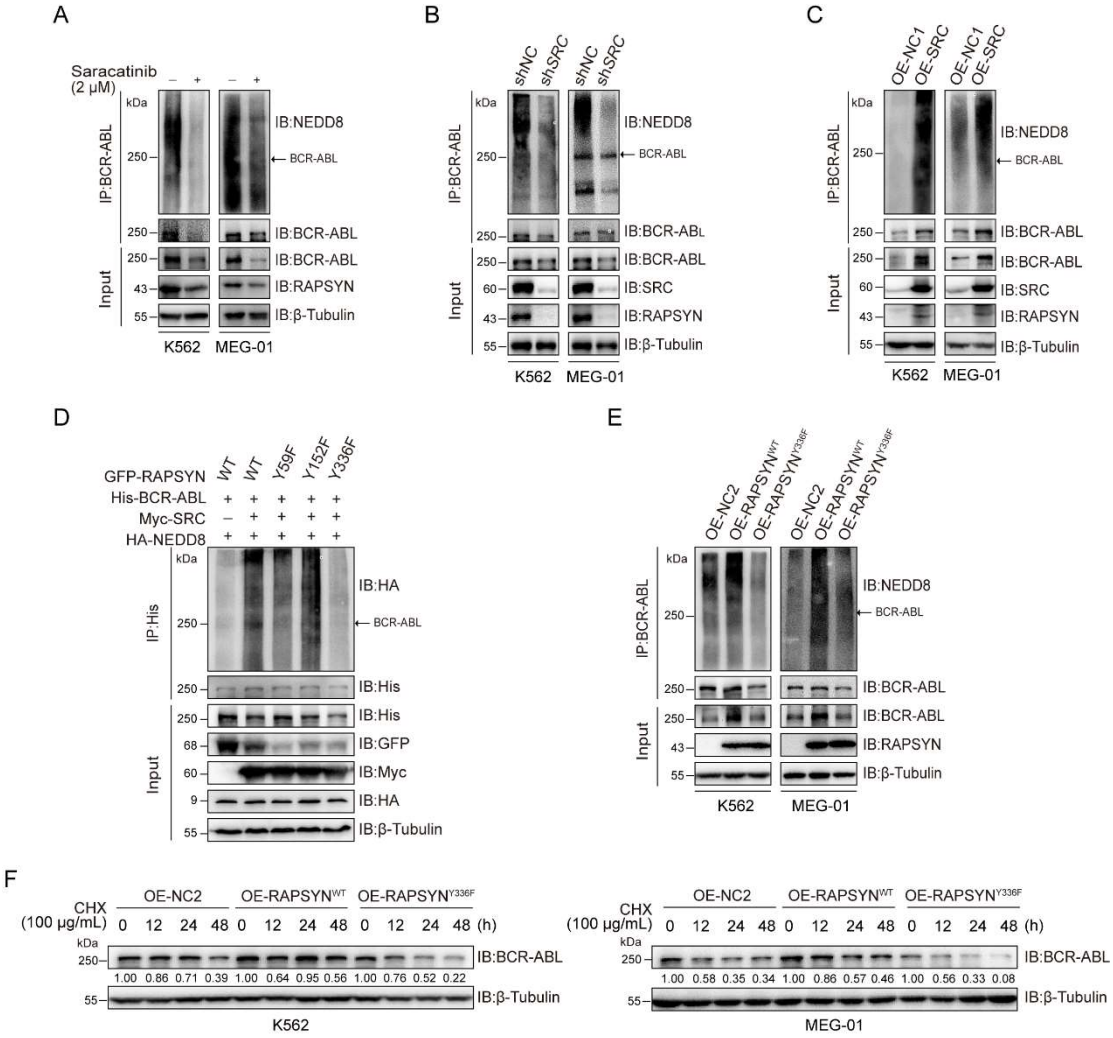


**Figure 5. RAPSYN phosphorylation at Y336 potentiates its E3 ligase activity and promotes BCR-ABL stabilization.**

(A) Immunoblots of BCR-ABL neddylation levels in leukemic cells treated with saracatinib or DMSO for 24 h.

(B) Immunoblots of BCR-ABL neddylation levels in leukemic cells transduced with sh*SRC* or shNC.

(C) Immunoblots of BCR-ABL neddylation levels in leukemic cells expressing exogenous SRC cDNA or empty vector.

(D) Effects of RAPSYN phosphorylation on BCR-ABL neddylation levels in HEK293T cells transfected with indicated constructs.

(E) Effects of RAPSYN phosphorylation at Y336 on BCR-ABL neddylation levels in leukemic cells expressing exogenous RAPSYN WT, Y336F cDNA, or empty vector.

(F) Assessment of BCR-ABL protein stability in leukemic cells transduced with exogenous cDNA for $RAPSYN^{WT}$, $RAPSYN^{Y336F}$ or empty vector by immunoblotting.

Figure 6

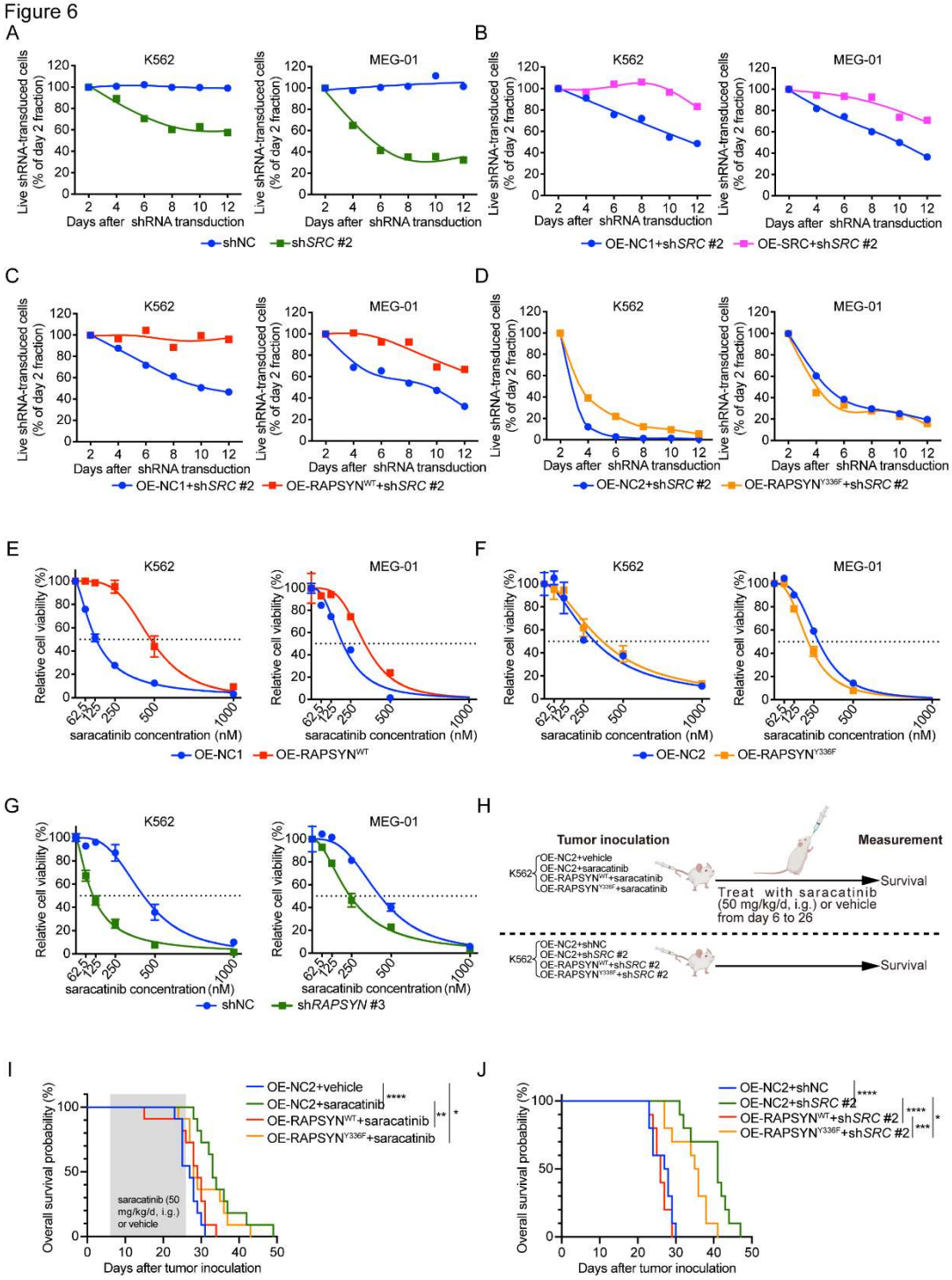


**Figure 6. SRC-mediated phosphorylation of RAPSYN at Y336 promotes Ph⁺ leukemia progression.**

(A) Cytotoxicity induced by sh*SRC* #2-mediated SRC knockdown in leukemic cells.

(B) Rescue of leukemic cells from sh*SRC* #2-induced toxicity by exogenous expression of SRC cDNA.

(C) Rescue of leukemic cells from sh*SRC* #2-induced toxicity by exogenous

855 expression of RAPSN$^{WT}$ cDNA.

856 (D) Failed rescue of leukemic cells from sh*SRC* #2-induced toxicity by exogenous
857 expression of RAPSN$^{Y336F}$ cDNA.

858 (E) Viability of leukemic cells transduced with either RAPSN$^{WT}$ cDNA or corresponding
859 empty vector after 72 h of incubation with indicated concentrations of saracatinib.

860 (F) Viability of leukemic cells transduced with either RAPSN$^{Y336F}$ cDNA or
861 corresponding empty vector after 72 h of incubation with indicated concentrations of
862 saracatinib.

863 (G) Viability of leukemic cells transduced with either shNC or sh*RAPSN* #3 after 72 h
864 of incubation with indicated concentrations of saracatinib.

865 (H) Experimental design used to test *in vivo* effects of RAPSYN phosphorylation at
866 Y336 on Ph$^{+}$ leukemia progression and survival time.

867 (I) Kaplan-Meier survival curve of NCG mice following intravenous injection of K562-
868 RAPSYN$^{WT}$ or K562-RAPSYN$^{Y336F}$ cells and intragastric administration of saracatinib
869 or corresponding vehicle from days 6 to 26 as indicated (ten mice in each group).

870 (J) Kaplan-Meier survival curve of NCG mice following intravenous injection of double-
871 transfected K562 cells (ten mice in each group). Representative results from at least
872 three independent experiments are shown (A-G); error bars, mean ± SD; * $p < 0.05$, **
873 $p < 0.01$, *** $p < 0.001$, **** $p < 0.0001$; log-rank test (I-L).

874

875

876

877

878

879

880

881

882

## References


Aydin, B., Kan, B., and Cabadak, H. 2013. The role of intracellular pathways in the proliferation of human K562 cells mediated by muscarinic receptors. *Leuk Res* ***37***: 1144-1149. DOI: 10.1016/j.leukres.2013.05.018.

Bahjat, M., de Wilde, G., van Dam, T., Maas, C., Bloedjes, T., Bende, R.J., van Noesel, C.J.M., Luijks, D.M., Eldering, E., Kersten, M.J., and Guikema, J.E.J. 2019. The NEDD8-activating enzyme inhibitor MLN4924 induces DNA damage in Ph+ leukemia and sensitizes for ABL kinase inhibitors. *Cell Cycle* ***18***: 2307-2322. DOI:10.1080/15384101.2019.1646068.

Barnes, D.J., Palaiologou, D., Panousopoulou, E., Schultheis, B., Yong, A.S., Wong, A., Pattacini, L., Goldman, J.M., and Melo, J.V. 2005. Bcr-Abl expression levels determine the rate of development of resistance to imatinib mesylate in chronic myeloid leukemia. *Cancer Res* ***65***: 8912-8919. DOI:10.1158/0008-5472.CAN-05-0076.

Bekes, M., Langley, D.R., and Crews, C.M. 2022. PROTAC targeted protein degraders: the past is prologue. *Nat Rev Drug Discov* ***21***: 181-200. DOI:10.1038/s41573-021-00371-6.

Braun, T.P., Eide, C.A., and Druker, B.J. 2020. Response and Resistance to BCR-ABL1-Targeted Therapies. *Cancer Cell* ***37***: 530-542. DOI:10.1016/j.ccell.2020.03.006.

Burslem, G.M., Schultz, A.R., Bondeson, D.P., Eide, C.A., Savage Stevens, S.L., Druker, B.J., and Crews, C.M. 2019. Targeting BCR-ABL1 in chronic myeloid leukemia by PROTAC-mmediated targeted protein degradation. *Cancer Res* ***79***: 4744-4753. DOI:10.1158/0008-5472.CAN-19-1236.

Cabadak, H., Aydin, B., and Kan, B. 2011. Regulation of M2, M3, and M4 muscarinic receptor expression in K562 chronic myelogenous leukemic cells by carbachol. *J Recept Signal Transduct Res* ***31***: 26-32. DOI:10.3109/10799893.2010.506484.

Cortes, J., Pavlovsky, C., and Saußele, S. 2021. Chronic myeloid leukaemia. *The Lancet* ***398***: 1914-1926. DOI:10.1016/s0140-6736(21)01204-6.

Deininger, M.W., Goldman, J.M., and Melo, J.V. 2000. The molecular biology of chronic myeloid leukemia. *Blood* ***96***: 3343-3356.

Demizu, Y., Shibata, N., Hattori, T., Ohoka, N., Motoi, H., Misawa, T., Shoda, T., Naito, M., and Kurihara, M. 2016. Development of BCR-ABL degradation inducers via the conjugation of an imatinib derivative and a cIAP1 ligand. *Bioorg Med Chem Lett* ***26***: 4865-4869. DOI:10.1016/j.bmcl.2016.09.041.

Durieux, M.E., and Nietgen, G.W. 1997. Synergistic inhibition of muscarinic signaling by ketamine stereoisomers and the preservative benzethonium chloride. *Anesthesiology* ***86***: 1326-1333. DOI:10.1097/00000542-199706000-00014.

Embade, N., Fernandez-Ramos, D., Varela-Rey, M., Beraza, N., Sini, M., Gutierrez de Juan, V., Woodhoo, A., Martinez-Lopez, N., Rodriguez-Iruretagoyena, B., Bustamante, F.J., de la Hoz, A.B., Carracedo, A., Xirodimas, D.P., Rodriguez, M.S., Lu, S.C., Mato, J.M., and Martinez-Chantar, M.L. 2012. Murine double minute 2 regulates Hu antigen R stability in human liver and colon cancer through NEDDylation. *Hepatology* ***55***: 1237-1248. DOI:10.1002/hep.24795.

Enchev, R.I., Schulman, B.A., and Peter, M. 2015. Protein neddylation: beyond cullin-RING ligases. *Nat Rev Mol Cell Biol* ***16***: 30-44. DOI:10.1038/nrm3919.

Guo, N., Azadniv, M., Coppage, M., Nemer, M., Mendler, J., Becker, M., and Liesveld, J. 2019. Effects of neddylation and mTOR Inhibition in acute myelogenous leukemia. *Transl Oncol* ***12***:

602-613. DOI:10.1016/j.tranon.2019.01.001.
Hochhaus, A., Baccarani, M., Silver, R.T., Schiffer, C., Apperley, J.F., Cervantes, F., Clark, R.E., Cortes, J.E., Deininger, M.W., Guilhot, F., Hjorth-Hansen, H., Hughes, T.P., Janssen, J., Kantarjian, H.M., Kim, D.W., Larson, R.A., Lipton, J.H., Mahon, F.X., Mayer, J., Nicolini, F., Niederwieser, D., Pane, F., Radich, J.P., Rea, D., Richter, J., Rosti, G., Rousselot, P., Saglio, G., Saussele, S., Soverini, S., Steegmann, J.L., Turkina, A., Zaritskey, A., and Hehlmann, R. 2020. European LeukemiaNet 2020 recommendations for treating chronic myeloid leukemia. *Leukemia* ***34***: 966-984. DOI:10.1038/s41375-020-0776-2.
Huh, K.H., and Fuhrer, C. 2002. Clustering of nicotinic acetylcholine receptors: from the neuromuscular junction to interneuronal synapses. *Mol Neurobiol* ***25***: 79-112. DOI:10.1385/MN:25:1:079.
Issaad, C., Ahmed, M., Novault, S., Bonnet, M.L., Bennardo, T., Varet, B., Vainchenker, W., and Turhan, A.G. 2000. Biological effects induced by variable levels of BCR-ABL protein in the pluripotent hematopoietic cell line UT-7. *Leukemia* ***14***: 662-670. DOI:10.1038/sj.leu.2401730.
Jabbour, E., Cortes, J., O'Brien, S., Giles, F., and Kantarjian, H. 2007. New targeted therapies for chronic myelogenous leukemia: opportunities to overcome imatinib resistance. *Semin Hematol* ***44***: S25-31. DOI:10.1053/j.seminhematol.2006.12.003.
Jabbour, E., and Kantarjian, H. 2020. Chronic myeloid leukemia: 2020 update on diagnosis, therapy and monitoring. *Am J Hematol* ***95***: 691-709. DOI:10.1002/ajh.25792.
Jakubik, J., Michal, P., Machova, E., and Dolezal, V. 2008. Importance and prospects for design of selective muscarinic agonists. *Physiol Res* ***57 Suppl 3***: S39-S47. DOI:10.33549/physiolres.931449.
Jiang, L., Wang, Y., Li, Q., Tu, Z., Zhu, S., Tu, S., Zhang, Z., Ding, K., and Lu, X. 2021a. Design, synthesis, and biological evaluation of Bcr-Abl PROTACs to overcome T315I mutation. *Acta Pharm Sin B* ***11***: 1315-1328. DOI:10.1016/j.apsb.2020.11.009.
Jiang, S., Wang, X., He, Y., Huang, H., Cao, B., Zhang, Z., Liu, J., Wang, Q., Huang, Z., and Mao, X. 2021b. Suppression of USP7 induces BCR-ABL degradation and chronic myelogenous leukemia cell apoptosis. *Cell Death Dis* ***12***: 456. DOI:10.1038/s41419-021-03732-6.
Bhalla KN, Fiskus W. 2016. NEDD8 and HDACs: promising cotargets in AML. *Blood* ***127***: 2167-2170. DOI:10.1182/blood-2016-02-699058.
Kawamata, J., Suzuki, S., and Shimohama, S. 2011. Enhancement of nicotinic receptors alleviates cytotoxicity in neurological disease models. *Ther Adv Chronic Dis* ***2***: 197-208. DOI:10.1177/2040622310397691.
Klein, A.d., Kessel, A.G.v., Grosveld, G., Bartram, C.R., Hagemeijer, A., Bootsma, D., Spurr, N.K., Heisterkamp, N., and J Groffen, J.R.S. 1982. A cellular oncogene is translocated to the Philadelphia chromosome in chronic myelocytic leukaemia. *Nature* ***300***: 765-767. DOI:10.1038/300765a0.
Lai, A.C., Toure, M., Hellerschmied, D., Salami, J., Jaime-Figueroa, S., Ko, E., Hines, J., and Crews, C.M. 2016. Modular PROTAC design for the degradation of oncogenic BCR-ABL. *Angew Chem Int Ed Engl* ***55***: 807-810. DOI:10.1002/anie.201507634.
Lee, G.W., Park, J.B., Park, S.Y., Seo, J., Shin, S.H., Park, J.W., Kim, S.J., Watanabe, M., and Chun, Y.S. 2018. The E3 ligase C-CBL inhibits cancer cell migration by neddylating the proto-oncogene c-Src. *Oncogene* ***37***: 5552-5568. DOI:10.1038/s41388-018-0354-5.
Legay, C., and Mei, L. 2017. Moving forward with the neuromuscular junction. *J Neurochem*

970 ***142 Suppl 2***: 59-63. DOI:10.1111/jnc.14028.
971 Li, J., Zou, J., Littlejohn, R., Liu, J., and Su, H. 2020. Neddylation, an emerging mechanism
972 regulating cardiac development and function. *Front Physiol* ***11***: 612927.
973 DOI:10.3389/fphys.2020.612927.
974 Li, L., Cao, Y., Wu, H., Ye, X., Zhu, Z., Xing, G., Shen, C., Barik, A., Zhang, B., Xie, X., Zhi, W.,
975 Gan, L., Su, H., Xiong, W.C., and Mei, L. 2016. Enzymatic activity of the scaffold protein rapsyn
976 for synapse formation. *Neuron* ***92***: DOI:1007-1019. 10.1016/j.neuron.2016.10.023.
977 Li, L., Xiong, W.C., and Mei, L. 2018. Neuromuscular junction formation, aging, and disorders.
978 *Annu Rev Physiol* ***80***: 159-188. 10.1146/annurev-physiol-022516-034255.
979 Li, X., and Song, Y. 2020. Proteolysis-targeting chimera (PROTAC) for targeted protein
980 degradation and cancer therapy. *J Hematol Oncol* ***13***: 50. DOI:10.1186/s13045-020-00885-3.
981 Liu, C., Nie, D., Li, J., Du, X., Lu, Y., Li, Y., Zhou, J., Jin, Y., and Pan, J. 2018. Antitumor effects
982 of blocking protein neddylation in T315I-BCR-ABL leukemia cells and leukemia stem cells.
983 *Cancer Res* ***78***: 1522-1536. DOI:10.1158/0008-5472.CAN-17-1733.
984 Liu, H., Mi, Q., Ding, X., Lin, C., Liu, L., Ren, C., Shen, S., Shao, Y., Chen, J., Zhou, Y., Ji, L.,
985 Zhang, H., Bai, F., Yang, X., Yin, Q., and Jiang, B. 2022. Discovery and characterization of
986 novel potent BCR-ABL degraders by conjugating allosteric inhibitor. *Eur J Med Chem* ***244***:
987 DOI:114810. 10.1016/j.ejmech.2022.114810.
988 Lussana, F., Intermesoli, T., Stefanoni, P., and Rambaldi, A. 2018. Mechanisms of resistance
989 to targeted therapies in chronic myeloid leukemia. *Handb Exp Pharmacol* ***249***: 231-250.
990 DOI:10.1007/164_2017_81.
991 Mao, J.H., Sun, X.Y., Liu, J.X., Zhang, Q.Y., Liu, P., Huang, Q.H., Li, K.K., Chen, Q., Chen, Z.,
992 and Chen, S.J. 2010. As4S4 targets RING-type E3 ligase c-CBL to induce degradation of BCR-
993 ABL in chronic myelogenous leukemia. *Proc Natl Acad Sci U S A* ***107***: 21683-21688.
994 DOI:10.1073/pnas.1016311108.
995 McGrail, D.J., Garnett, J., Yin, J., Dai, H., Shih, D.J.H., Lam, T.N.A., Li, Y., Sun, C., Li, Y.,
996 Schmandt, R., Wu, J.Y., Hu, L., Liang, Y., Peng, G., Jonasch, E., Menter, D., Yates, M.S., Kopetz,
997 S., Lu, K.H., Broaddus, R., Mills, G.B., Sahni, N., and Lin, S.Y. 2020. Proteome instability is a
998 therapeutic vulnerability in Mismatch Repair-Deficient cancer. *Cancer Cell* ***37***: 371-386 e312.
999 DOI:10.1016/j.ccell.2020.01.011.
1000 Mohamed, A.S., and Swope, S.L. 1999. Phosphorylation and cytoskeletal anchoring of the
1001 acetylcholine receptor by Src class protein-tyrosine kinases. Activation by rapsyn. *J Biol Chem*
1002 ***274***: 20529-20539. DOI:10.1074/jbc.274.29.20529.
1003 Norton, J.P., Augert, A., Eastwood, E., Basom, R., Rudin, C.M., and MacPherson, D. 2021.
1004 Protein neddylation as a therapeutic target in pulmonary and extrapulmonary small cell
1005 carcinomas. *Genes Dev* ***35***: 870-887. DOI:10.1101/gad.348316.121.
1006 Önder Narin G., Aydin, B., and Cabadak, H. 2021. Studies on the role of alpha 7 nicotinic
1007 acetylcholine receptors in K562 cell proliferation and signaling. *Mol Biol Rep* ***48***: 5045-5055.
1008 DOI:10.1007/s11033-021-06498-4.
1009 Oved, S., Mosesson, Y., Zwang, Y., Santonico, E., Shtiegman, K., Marmor, M.D.,
1010 Kochupurakkal, B.S., Katz, M., Lavi, S., Cesareni, G., and Yarden, Y. 2006. Conjugation to
1011 Nedd8 instigates ubiquitylation and down-regulation of activated receptor tyrosine kinases. *J*
1012 *Biol Chem* ***281***: 21640-21651. DOI:10.1074/jbc.M513034200.
1013 Shibata, N., Ohoka, N., Tsuji, G., Demizu, Y., Miyawaza, K., Ui-Tei, K., Akiyama, T., and Naito,

1014 M. 2020. Deubiquitylase USP25 prevents degradation of BCR-ABL protein and ensures
1015 proliferation of Ph-positive leukemia cells. *Oncogene* ***39***: 3867-3878. DOI:10.1038/s41388-
1016 020-1253-0.
1017 Shimokawa, K., Shibata, N., Sameshima, T., Miyamoto, N., Ujikawa, O., Nara, H., Ohoka, N.,
1018 Hattori, T., Cho, N., and Naito, M. 2017. Targeting the allosteric site of oncoprotein BCR-ABL
1019 as an alternative strategy for effective target protein degradation. *ACS Med Chem Lett* ***8***: 1042-
1020 1047. DOI:10.1021/acsmedchemlett.7b00247.
1021 van der Veen, A.G., and Ploegh, H.L. 2012. Ubiquitin-like proteins. *Annu Rev Biochem* ***81***: 323-
1022 357. DOI:10.1146/annurev-biochem-093010-153308.
1023 Wang, S., Xie, W., Wang, D., Peng, Z., Zheng, Y., Liu, N., Dai, W., Wang, Y., Wang, Z., Yang,
1024 Y., and Chen, Y. 2015. Discovery of a small molecule targeting SET-PP2A interaction to
1025 overcome BCR-ABL$^{T315I}$ mutation of chronic myeloid leukemia. *Oncotarget* ***6***: 12128-12140.
1026 DOI:10.18632/oncotarget.3665.
1027 Witzemann, V., Chevessier, F., Pacifici, P.G., and Yampolsky, P. 2013. The neuromuscular
1028 junction: selective remodeling of synaptic regulators at the nerve/muscle interface. *Mech Dev*
1029 ***130***: 402-411. DOI:10.1016/j.mod.2012.09.004.
1030 Xie, P., Peng, Z., Chen, Y., Li, H., Du, M., Tan, Y., Zhang, X., Lu, Z., Cui, C.P., Liu, C.H., He, F.,
1031 and Zhang, L. 2021. Neddylation of PTEN regulates its nuclear import and promotes tumor
1032 development. *Cell Res* ***31***: 291-311. DOI:10.1038/s41422-020-00443-z.
1033 Xing, G., Jing, H., Zhang, L., Cao, Y., Li, L., Zhao, K., Dong, Z., Chen, W., Wang, H., Cao, R.,
1034 Xiong, W.C., and Mei, L. 2019. A mechanism in agrin signaling revealed by a prevalent Rapsyn
1035 mutation in congenital myasthenic syndrome. *eLlife* ***8***. DOI:10.7554/eLife.49180.
1036 Xing, G., Xiong, W.C., and Mei, L. 2020. Rapsyn as a signaling and scaffolding molecule in
1037 neuromuscular junction formation and maintenance. *Neurosci Lett* ***731***: 135013.
1038 DOI:10.1016/j.neulet.2020.135013.
1039 Yang, Y., Ding, L., Guo, Z.K., Zheng, X.L., Wang, L.S., Sun, H.Y., Jin, Z.G., and Wang, H.X.
1040 2017. The epigenetically-regulated miR-34a targeting c-SRC suppresses RAF/MEK/ERK
1041 signaling pathway in K-562 cells. *Leuk Res* ***55***: 91-96. DOI:10.1016/j.leukres.2017.01.020.
1042 Yao, J., Liang, X., Liu, Y., and Zheng, M. 2020. Neddylation: A Versatile Pathway Takes on
1043 Chronic Liver Diseases. *Front Med (Lausanne)* ***7***: 586881. DOI:10.3389/fmed.2020.586881.
1044 Ying, J., Zhang, M., Qiu, X., and Lu, Y. 2018. Targeting the neddylation pathway in cells as a
1045 potential therapeutic approach for diseases. *Cancer Chemother Pharmacol* ***81***: 797-808.
1046 DOI:10.1007/s00280-018-3541-8.
1047 Zhao, Q., Ren, C., Liu, L., Chen, J., Shao, Y., Sun, N., Sun, R., Kong, Y., Ding, X., Zhang, X.,
1048 Xu, Y., Yang, B., Yin, Q., Yang, X., and Jiang, B. 2019. Discovery of SIAIS178 as an effective
1049 BCR-ABL degrader by recruiting Von Hippel-Lindau (VHL) E3 ubiquitin ligase. *J Med Chem* ***62***:
1050 9281-9298. 10.1021/acs.jmedchem.9b01264.
1051 Zhou, L., Chen, S., Zhang, Y., Kmieciak, M., Leng, Y., Li, L., Lin, H., Rizzo, K.A., Dumur, C.I.,
1052 Ferreira-Gonzalez, A., Rahmani, M., Povirk, L., Chalasani, S., Berger, A.J., Dai, Y., and Grant,
1053 S. 2016. The NAE inhibitor pevonedistat interacts with the HDAC inhibitor belinostat to target
1054 AML cells by disrupting the DDR. *Blood* ***127***: 2219-2230. DOI:10.1182/blood-2015-06-653717.
1055 Zhou, L., Jiang, Y., Luo, Q., Li, L., and Jia, L. 2019. Neddylation: a novel modulator of the tumor
1056 microenvironment. *Mol Cancer* ***18***: 77. DOI:10.1186/s12943-019-0979-1.
1057 Zhou, Q., and Sun, Y. 2019. MLN4924: additional activities beyond neddylation inhibition. *Mol*

1058 *Cell Oncol* ***6***: e1618174. DOI:10.1080/23723556.2019.1618174.
1059 Zuo, W., Huang, F., Chiang, Y.J., Li, M., Du, J., Ding, Y., Zhang, T., Lee, H.W., Jeong, L.S.,
1060 Chen, Y., Deng, H., Feng, X.H., Luo, S., Gao, C., and Chen, Y.G. 2013. c-Cbl-mediated
1061 neddylation antagonizes ubiquitination and degradation of the TGF-beta type II receptor. *Mol*
1062 *Cell* ***49***: 499-510. DOI:10.1016/j.molcel.2012.12.002.
1063